A POROUS MEDIA APPROACH TOWARDS A DYNAMIC MECHANISTIC MODEL OF DRUG ELIMINATION BY THE LIVER

A Thesis Submitted to the

College of Graduate Studies and Research

in Partial Fulfillment of the Requirements

for the Degree of Master of Science in the

Division of Biomedical Engineering

University of Saskatchewan

Saskatoon, Saskatchewan

By

MOHAMMAD IZADIFAR

PERMISSION TO USE

In presenting this thesis in partial fulfillment of the requirements for a Postgraduate degree from the University of Saskatchewan, I agree that the Libraries of this University may make it freely available for inspection. I further agree that permission for copying of this thesis in any manner, in whole or in part, for scholarly purposes may be granted by the professor or professors who supervised my thesis work or, in their absence, by the Head of the Department or the Dean of the College in which my thesis work was done. It is understood that any copying or publication or use of this thesis or parts thereof for financial gain shall not be allowed without my written permission. It is also understood that due recognition shall be given to me and to the University of Saskatchewan in any scholarly use which may be made of any material in my thesis.

Requests for permission to copy or to make other uses of materials in this thesis in whole or part should be addressed to:

Head of the Division of Biomedical Engineering

University of Saskatchewan

Saskatoon, Saskatchewan S7N 5A9

Canada

ABSTRACT

Hepatic drug elimination is a major PK process contributing to loss of drug concentration in the body. The prediction of hepatic clearance (and hence drug concentrations in the body) requires an understanding of the physiology and mechanisms of the hepatic elimination process and their compilation into a mechanistic model. Several physiological models including well-stirred model, parallel tube model and dispersion model have been developed to describe the hepatic elimination process and to determine how physiological variables such as blood flow, unbound fraction and enzyme activity may influence the hepatic clearance. However, each model has distinguishing advantages and limitations, which lead sometimes to very disparate prediction outcomes. Although hepatic drug elimination has been mathematically described by different physiological models, the mass transfer phenomena in the liver has not been described from a porous media viewpoint using local volume averaging method. The inherently porous structure of the liver allows us to describe the hepatic drug elimination process based on a porous media approach such that structural properties of the liver tissue, physico-chemical properties of the drug as well as transport properties associated with the hepatic blood perfusion are included in the model.

Applying local volume averaging method and local equilibrium to the liver as a porous medium, a governing partial differential equation which takes into account liver porosity, tortuosity, permeability, unbound drug fraction and hepatic tissue partition coefficient, drug-plasma diffusivity, axial/radial dispersion and hepatocellular metabolism parameters was developed. The governing equation was numerically solved using implicit finite difference and Gauss-Seidel iterative method in order to describe changes in dug concentration with time and position across the liver following an intravenous drug administration. The model was used to

predict hepatic clearance and bioavailability, which were then compared to reported observations.

The predicted values of hepatic clearance and bioavailability had good agreement with the reported observations for high and low clearance drugs. As well, the model was able to successfully predict an unsteady state of hepatic drug elimination with concentration dependent intrinsic clearance. When statistically compared to the well-stirred, parallel tube and dispersion models the proposed model suggested a smaller mean squared prediction error and very good agreement to reported observations for eight drugs. A sensitivity analysis revealed that an increase in liver porosity results in a slight decrease in the drug concentration gradient across the liver while higher tissue partition coefficient values increase the concentration gradient. The model also suggested that the bioavailability was sensitive to the interaction between unbound fraction and intrinsic clearance. This study indicates that the liver and hepatic drug elimination can be successfully explored from a porous media viewpoint and may provide better mechanistic predictions of drug elimination processes by the liver.

ACKNOWLEDGMENTS

First of all, I would like to thank God, the Almighty, for having made everything possible by giving me strength and courage to do this work.

I would like to gratefully acknowledge Dr. Oon-Doo Baik, my supervisor, for unflinching supports in various ways during my study. As well, I would like to record my deepest gratitude to Dr. Jane Alcorn, my advisor from the division of Pharmacy, for guidance, encouragement and valuable comments. I appreciate comments and the time spent on reviewing the drafts of this thesis by Dr. Daniel Chen, my GAC chair. I am also thankful to Dr. David M. Janz for serving as the external examiner and for his constructive comments on the draft of this thesis.

Finally, sincere and infinite thanks go to my dearests, my father and mother for their patience and encouragement during my study abroad; the patience and encouragement that I really appreciate.

TABLE OF CONTENTS

LIST OF FIGURES

LIST OF TABLES

NOMENCLATURE

A	Cross sectional area (m^2)
a	Parameters in Eqs. (1.24), (1.29) and (2.15)
C_A	Arterial blood drug concentration (mg/ml)
C_b	Total blood drug concentration (mg/ml)
C	Drug concentration (mg/ml)
$< C >^P$	Local volume average plasma drug concentration (mg/ml)
C_p	Plasma drug concentration (mg/ml)
C_{ss}	Steady state plasma drug concentration (mg/ml)
C_u	Unbound drug concentration (mg/ml)
C_V	Venous blood drug concentration (mg/ml)
Cl_H	Hepatic clearance (ml/s)
Cl_{h_DP}	Hepatic clearance from dispersion model (ml/s)
Cl_{h_LVA}	Local volume averaged hepatic clearance (ml/s)
Cl_{h_PT}	Hepatic clearance from parallel tube model (ml/s)
Cl_{h_WS}	Hepatic clearance from well stirred model (ml/s)
Cl_{in_invivo}	Invivo intrinsic clearance (1/s)
$Cl_{in\text{-}overall}$	Overall hepatic intrinsic clearance (ml/s)
Cl_{int}	Intrinsic clearance (ml/s)
Cl_{organ}	Organ clearance (ml/s)
Cl_s	Systemic clearance (ml/s)
D_{AB}	Drug-plasma molecular diffusion coefficient (m^2/s)
$D_{\parallel}^{d}$	Axial dispersion coefficient (dimensionless)
$D_{\perp}^{d}$	Radial dispersion number (dimensionless)
d_p	Pore size (m)
D_n	Dispersion number (dimensionless)
dV	Differential volume (ml)
ER	Extraction ratio (dimensioless)
F	Bioavailability (dimensionless)
F_H	Hepatic bioavailability (dimensionless)

$f_{u(B)}$	Unbound drug concentration (dimensionless)
H	Hematocrit (dimensionless)
i	Node number index (dimensionless)
j	Time step index (dimensionless)
K	Tissue hydraulic conductivity (m^2)
K^*	Tissue partition coefficient (dimensionless)
$\mathbf{K_e}$	Diagonal matrix of elimination rate constant (1/s)
K_M	Affinity term (mg/ml)
k_{phys}	Sinusoidal based permeability (m^2)
L	Length (m)
l	Representative elementary volume length scale (m)
$\mathbf{M}$	The matrix coefficient of the mass exchange (1/s)
MRT	Mean residence time of the drug in the body (s)
$\hat{m}_{met}$	Local volume averaged hepatocellular metabolism rate (mg/ml.s)
N	Number of nodes or compartments (dimensionless)
Pe	Peclet number (dimensionless)
$PS_{u,efflux}$	Efflux membrane permeability of unbound drug (ml/s)
$PS_{u,influx}$	Influx membrane permeability of unbound drug (ml/s)
ΔP	Pressure drop (Pas.)
Q	Blood perfusion rate (ml/s)
Q_h	Hepatic perfusion rate (ml/s)
t	Time (s)
Δt	Time step size (s)
u	Linear velocity (m/s)
$\overline{u}_B$	Blood Darcy velocity (m/s)
$\mathbf{V}$	Diagonal matrix of blood velocity (m/s)
V	Volume (ml)
V_d	Volume of distribution (ml)
V_{max}	Maximum enzyme activity capacity (mg/ml s)
V_{ss}	Steady state volume of distribution (ml)

V_t	Tissue volume (ml)
W_b	Body weight (kg)
x	Position (m)
X_{IV}	Intravascular dose of the drug (mg)
X_0	Dose (mg)
Δx	Mesh size (m)
Z	Dimensionless position along the liver (dimensionless)
z	Position (m)

Greek letters

α	Parameter in Eqs. (2.20) to (2.23)
β	Parameter in Eqs. (2.20) to (2.23)
ε	Porosity (dimensionless)
$<\varphi>$	Local volume average property
γ	Parameter in Eqs. (2.20) to (2.23)
μ	Viscosity (kg/m s)
θ	Parameter in Eqs. (2.20) to (2.23)
τ	Tortuosity (dimensionless)
ϑ	Hepatocellular metabolism rate (mg/s)
ω	Elimination rate (mg/s)
ζ	Heterogeneity coefficient (dimensionless)

CHAPTER 1

BACKGROUND AND LITERATURE REVIEW

1.1 Introduction

Physiological modeling contributes substantially to drug discovery and development through its ability to provide better insight into mechanisms and processes attributed to pharmacokinetics (PK) and integrate these with pharmacodynamic (PD) processes. A mechanistic model which can adequately describe *in-vivo* physiological phenomena based on limited available *in-vitro* data can reduce the costs of animal experiments and loss in time due to poor selection of possible lead candidates. Such a model can perform sensitivity analyses to estimate expected PK profiles of new drugs in human. However, a reduction in prediction uncertainties only follow from the avoidance of oversimplifications or assumptions that often exclude critical determinants of the PK properties of a compound. Today, pharmaceutical companies focus efforts on developing more predictive models to describe the physiological processes more precisely so that the animal experiments can be reduced, refined and replaced by mathematical models. In addition, developing predictive physiological/mechanistic models are required for better understanding and analyzing pathophysiological events in the body.

Hepatic drug elimination is a major PK process contributing to loss of drug concentration in the body. The prediction of hepatic clearance (and hence drug concentrations in the body) requires an understanding of the physiology and mechanisms of the hepatic elimination process and their compilation into a mechanistic model. Several physiological models, namely the well-

stirred (WS) model, parallel tube (PT) model and dispersion (DP) model, have been developed to describe the hepatic elimination process and to determine how physiological variables such as blood flow, unbound fraction and enzyme activity may influence the hepatic clearance. However, each model has distinguishing advantages and limitations, which lead sometimes to very disparate prediction outcomes.

Simplifications and assumptions which are made to develop and solve models are the major sources of uncertainties of predictions. To improve the predictability of a mechanistic model for hepatic drug elimination, the mathematical formulation must be consistent with the physiological and physical phenomena taking place in the liver. In the WS model, drug is assumed to be instantaneously and homogeneously mixed with the blood in the liver resulting in very uniform drug concentration across the liver. This idealized oversimplification adds important associated uncertainties in predictions by the WS model. Furthermore, the WS model ignores the concentration gradient across the liver which is contradictory to realistic phenomenon in the liver. Although the PT and DP models assume an exponential drug concentration gradient across the liver, these models do not take into account the influence of liver structural characteristics such as tissue porosity and tortuosity and tissue partition coefficients. The DP model has an advantage over PT model by taking into account the dispersion mechanism of the drug transport in the liver; however, DP model assumes that the hepatocellular metabolism rate is constant such that the drug concentration in hepatocytes is independent of time, and physico-chemical properties remain unchanged with the position across the liver. In reality, enzyme activity changes with the drug concentration across the liver and the drug concentration in hepatocytes as well as physico-chemical properties can change with time.

An ability to make robust predictions of drug elimination by the liver requires a mechanistic model that simulates real physiological events in the liver. This study focuses on the development and validation of a mechanistic model that represents the liver's structural properties based on the concepts of porous media and considers unsteady state properties in the liver and concentration dependent metabolic intrinsic clearance (the inherent ability of liver cells to eliminate the drug) and transport mechanisms of a drug.

1.2 The liver's central role in ADME processes

Absorption, distribution, metabolism and excretion (ADME) of a drug are the major processes which are quantitatively discussed in pharmacokinetics (PK). Together with physiological and pharmacodynamics properties, ADME processes determine the therapeutic profile of a drug. For example, if a drug compound is poorly absorbed in the intestine and is highly metabolized in the liver or rapidly excreted by the kidneys, the drug will be unable to provide its optimum therapeutic effects so that higher dose levels of the drug will be required to achieve sufficient drug concentration in the target organ for full therapeutic effect of the drug (Yanni and Thakker, 2007). Also, if the drug is poorly lipophilic, drug distribution in a target tissue i.e. brain will be so poor that the drug efficacy will be low despite its high plasma drug concentration. Therefore, it is very important to understand and quantify ADME processes.

Among ADME processes, hepatic drug metabolism is considered as an important process for drug elimination from the body and can be an important determinant of plasma drug concentrations. The liver is the major site of drug metabolism in the body and is responsible for blood detoxification whereby toxic substances in the blood are metabolized by the liver with the same principles as drug elimination processes. The liver is also a principal organ in the

maintenance of homeostasis. In order to understand the role of the liver in drug PK then, requires a knowledge of PK concepts and parameters, drug physico-chemical properties and liver anatomy, architecture and physiology.

1.2.1 Systemic circulation

The systemic circulation supplies blood to all tissues throughout the body except for the pulmonary circulation which has its inclusive blood circulation system. The contraction of heart's left ventricle forcefully pushes the fully oxygenated blood through the aorta which branches into many small arteries and further into arterioles and terminating into capillary beds throughout organs and tissues of the body. Arteries, arterioles and capillaries are responsible for oxygen and nutrient delivery to the tissues. Oxygen, nutrients, drug compounds as well as any possible toxic substances are transferred from capillaries to the tissues while wastes are transferred back into the capillaries which conduct the low oxygenated blood to the heart through venules which collect into larger vessels, the veins. Then the pulmonary circulation system takes over oxygenating the blood in lungs.

In the systemic circulation, the heart supplies the oxygenated blood to the whole body via the arterial blood supply. The oxygenated blood is distributed in tissues and organs where the oxygen, nutrients and/or drug compounds are exchanged within tissue capillary beds. The various organs and tissues of the body receive a fraction of the cardiac output in parallel. Also, the blood passes through the portal circulation around the gastrointestinal tract from which nutrients as well as drug compounds are absorbed from the intestine into the portal blood. The serial nature of the blood supply from gastrointestinal tract through the portal vein to the liver and hepatic vein distinguishes the portal vein blood supply over the parallel nature of blood distribution in major organs in the body. Portal vein directs the nutrient enriched blood to the liver where the blood is mixed with the hepatic arterial blood in sinusoids and eventually is

drained into the hepatic vein. The hepatic vein joins the veins from the rest of the body towards the heart where deoxygenated blood is pumped to the pulmonary circulation.

1.2.2 Distribution concepts

The distribution process is defined as the reversible movement of drug between the systemic circulation and tissues of the body. The reversible drug distribution between the blood and tissues can be characterized by the rate of distribution and the extent of distribution. Although the rate of drug distribution is important, the extent of drug distribution is considered as a key PK process. Tissue perfusion rate, the permeability of tissue membranes, the drug binding ability with the blood proteins and tissue, and the lipophilicityof the drug can influence the extent and the rate of drug distribution.

1.2.2.1 Volume of distribution

Blood volume in human body is variable but roughly it can be approximated as much as 8% of the body weight. An average adult has about 5 L blood in the body. Unlike the definition of volume in chemical reaction engineering where a compound is distributed throughout a fixed volume, in pharmacokinetics the available space for a drug compound distribution in the body can change due to the disease state, physiological condition and physico-chemical properties of the drug. Therefore, a different measure is required to well define the space in which the drug is distributed in the body (Benet, 2010). Volume of distribution is the measure that describes the apparent volume into which a drug distributes in the body at equilibrium condition. This important PK has no physiological reality, rather represents a fictitious volume to identify the extent of drug distribution in tissues. Theoretically the distribution of a drug cannot exceed the total body water (vascular fluid, extracellular and intracellular fluid); however, depending on the physico-chemical properties of the drug (i.e. protein binding), disease state and physiological conditions, the volume of distribution can be smaller or much larger than the total body water

volume. For example, if the drug is poorly plasma protein bound, it is highly distributed in the body tissues rather than the plasma; therefore, the apparent volume of distribution will be larger than the blood volume in the body. The apparent volume of distribution is a proportionality ratio calculated by definition as:

$$V_d = \frac{X_{IV}}{C_p} \tag{1.1}$$

where V_d is the apparent volume of distribution (L), X_{IV} is the intravascular (IV) dose (mg) and C_p is the plasma concentration at distribution equilibrium (mg/L).

The volume of distribution is independent of drug elimination. Since systemic clearance (see section 1.2.3), which is the measure of elimination efficiency, and volume of distribution are basically independent of each other, the volume of distribution at steady state can be defined based on the mean residence time (*MRT*) of the drug in the body as (Benet, 2010):

$$V_{ss} = Cl_s \times MRT \tag{1.2}$$

where V_{ss} is the volume of distribution at steady state (L), Cl_s is systemic clearance (L/h) and *MRT* is the mean residence of the drug in the body (h).

Conceptually, the volume of distribution depends on several physiological determinants including blood volume, blood flow, partition coefficient (see section 1.2.2.3) and protein binding. The greater the blood volume and a larger blood flow in a tissue allows a larger amount of drug to be available to the tissue and a rapid drug presentation to the tissue. These factors enhance the extent and the rate of the drug distribution in the tissue. Also, increased drug lipophilicity results in a larger drug partitioning in the tissue. Increased lipophilicity can lead to more extensive distribution of the drug in the tissue in the presence of sufficiently high blood flow and volume in the tissue. When the equilibrium between the plasma and the tissue is

established, the unbound fraction of the drug in the tissue can influence the volume of distribution. Larger unbound fraction of the drug in the tissue leads to the drug transfer from the tissue to the plasma and it reduces the extent of drug distribution in the tissue.

1.2.2.2 Blood protein binding and unbound fraction

A drug can undergo binding to different blood constitutes including red blood cells, white blood cells and plasma proteins. Therefore, different kinds of drug concentration can be defined as blood drug concentration, plasma drug concentration and unbound drug concentration. In terms of PK processes the only fraction of drug available for crossing biological membranes is the free or unbound drug in blood. Therefore, increases in the unbound drug fraction (ratio of unbound drug concentration to total drug concentration) results in greater distribution of drug into tissues, which increases the volume of distribution. Due to the highly significant variability of plasma protein binding, a large variation in the volume of distribution can be observed for a single drug. In addition, diseases and drug-drug interactions can influence the plasma protein binding of a drug which consequently alters the volume of distribution of the drug.

The clinical term of drug unbound fraction is defined as the ratio of the unbound drug concentration to the total drug concentration. If the unbound fraction of a drug is smaller than 0.1, the drug will be considered highly protein bound and sensitive to changes in protein binding; however, if the unbound fraction is larger than 0.8, clinically any changes in protein binding can lead to insignificant influences on disposition and elimination processes (see section 1.2.5.1.3).

Another measure which describes the extent of binding of a drug in the blood cells is blood-to-plasma concentration ratio which is defined as the ratio of the drug concentration in blood cells to that in unbound plasma. Since hematocrit is defined as the volumetric fraction of blood

cells with respect to the blood volume, the blood-to-plasma concentration ratio can be formulated by definiation as:

$$\psi = \frac{H - 1 + \left(\frac{C_b}{C_p}\right)}{f_{u(B)} H} \tag{1.3}$$

where H is hematocrit, C_b is the total blood drug concentration, C_p is the plasma drug concentration, $f_{u(B)}$ is the unbound fraction and ψ is the blood-to-plasma concentration ratio.

1.2.2.3 Equilibrium and tissue partition coefficient

Drugs can be hydrophilic (soluble in plasma water and extra-intracellular fluids) or lipophilic (plasma protein bound) in nature. Most lipophilic drug compounds exhibit reversible protein binding interactions involving weaker chemical bonds with proteins. Within the plasma or a tissue compartment, lipophilic drugs undergo reversible binding with the active sites of the proteins to reach an equilibrium between bound and unbound drug molecules. The equilibrium conditions determine the plasma unbound drug concentration which is the only form of drug molecules to traverse the membrane and diffuse into tissues.

The migration of plasma unbound drug molecules to the tissue depends on the degree of lipophilicity of molecules and the rate of presentation of drugs to the tissue by the blood flow. For high lipophilic drugs, the limiting factor is the blood flow while for low lipophilic with low solubility in the membrane the plasma-tissue exchanged is a diffusion limited process (Levitt, 2010). The extent of the drug partitioning between the plasma and the tissue can be represented by the physiological measure of partition coefficient. Partition coefficient is defined as the ratio of drug concentration in the tissue to the unbound drug concentration in plasma when the tissue and the plasma are in equilibrium. Providing sufficiently high blood flow rate, the drug partition coefficient can be used for determination of the extent of drug distribution in a tissue; however,

partition coefficient is unable to evaluate how quickly the drug compound is distributed in the tissue. The rate of drug distribution in a tissue relies on the perfusion rate and the diffusivity of the drug across the membrane.

1.2.3 Systemic clearance concepts

After a drug compound reaches the systemic circulation, it is distributed in tissues and organs some of which eliminate the drug compound from the body. Drugs are mostly eliminated from the body either in unchanged form (parent drug) or changed form (metabolized drug). Depending on the water solubility or lipophilicity, the drug can be excreted by the kidneys or be metabolized by the liver. The kidney is the most important organ for excretion of polar drugs and their metabolites; however excretion may also occur via the lungs, skin, milk and bile. Liver is the major elimination organ responsible for the metabolism of lipophilic drugs and converting them into water soluble metabolites which are excreted through the kidneys. Biliary excretion of parent drug or metabolites may occur with a potential for their reabsorption from the intestine. In order to describe the efficiency of the elimination process by the major elimination organs, liver and kidney, a physiological measure of clearance is defined. The concept of the clearance was originally introduced by Rowland et al. (1973). Total body clearance or systemic clearance is defined as the volume of the blood cleared of drug per unit time in the body. Hepatic and renal clearance are defined as the volume of the blood cleared from the drug per unit time by the liver and kidneys, respectively.

1.2.3.1 Elimination rate and extraction ratio

The systemic clearance at steady state can be calculated based on the steady state drug plasma concentration (C_{ss}), availability of the drug in the blood (F), administration interval (τ) and the dose (X_0) as follows (Rowland et al., 1973):

$$Cl_s = \frac{FX_0 / \tau}{C_{ss}} \tag{1.4}$$

Rowland et al. (1973) and Wilkinson and Shand (1975) introduced the concept of organ elimination rate defined as the product of the blood flow rate by the drug concentration difference between the arterial and venous blood of the organ as:

$$\omega = Q(C_A - C_V) \tag{1.5}$$

ω is the elimination rate, Q is the perfusion rate to the elimination organ, C_A and C_V are the drug concentrations in arterial and venous blood, respectively. Dividing Eq. (1.5) by the arterial drug concentration leads to the following equation describing the organ clearance as:

$$Cl_{organ} = \frac{Q(C_A - C_V)}{C_A} \tag{1.6}$$

where $(C_A\text{-}C_V)/C_A$ is called the extraction ratio (ER) and defined as the fraction of arterial drug eliminated by the organ. The ER is basically a function of blood perfusion rate of the organ, the intrinsic ability of the organ to eliminate the drug, and the unbound fraction of the drug in the blood.

Borrowing the concept of well stirred reactor model, Wilkinson and Shand (1975) assumed the liver as a homogenous reactor vessel in order to incorporate the above physiological factors into the conceptual definition of hepatic clearance. A physiologically defined hepatic clearance was then introduced as:

$$Cl_H = \frac{Qf_{u(B)}Cl_{int}}{Q + f_{u(B)}Cl_{int}} \tag{1.7}$$

where Cl_H is the hepatic clearance and Cl_{int} is the intrinsic clearance representing the maximum enzymatic metabolism capacity of the liver. Hepatic clearance has the central role in eliminating

lipophilic drugs. As it was discussed, the cell membranes are lipid in nature and lipid soluble drugs can readily traverse the membranes of tissue cells. In the same way, lipophilic drugs can easily enter the liver cells and undergo hepatic metabolism the efficiency of which is given by the hepatic clearance.

1.2.3.2 Administration routes and pre-systemic elimination

Drug administration can be performed through different extravascular routes, such as oral, rectal, subcutaneous, intramuscular, or intravascular administrations. Depending on the site of administration, the fraction of the drug that reaches the systemic circulation (i.e. bioavailability) can vary. Figure 1.1 illustrates a schematic diagram of the blood circulation system and the major sites of the drug administration. Administration sites 1 and 2 represent IV administration sites, and site 3 indicates the gastrointestinal absorption of a drug administered orally. As it can be seen, after the blood is circulated through the pulmonary circulation, it is pumped into the systemic circulation while the oxygenated blood is directed to the gastrointestinal tract where drug and nutrient absorption takes place. Then the blood perfuses the liver where drug metabolism occurs. The blood leaving the liver through the hepatic vein joins the venous blood coming from the general circulation in body and is conducted towards the heart. If the drug is administered at Site 1, providing that the lung has no contribution to the drug elimination, sampling from the vein associated with the general circulation can lead to a good estimation of systemic clearance. Likewise, if the drug is administered at Site 2 representing intra-arterial administration, it will be distributed in the body during its first passage without undergoing any elimination process. However, oral administration of a drug is followed by drug absorption in gastrointestinal tract, Site 3. If the administration occurs at Site 3, the drug is absorbed into the portal vein that directs the blood to the liver. The portal blood containing the drug compound

perfuses the liver where a fraction of the drug is metabolized before it reaches the systemic circulation. Elimination during the first passage of the drug through the liver is called the first pass effect which causes an error in the estimation of systemic clearance. In addition, the drug may be subjected to metabolism in gastrointestinal tract lumen, gastrointestinal tract mucosa, the intestinal and the portal vein further reducing the fraction of parent drug reaching the systemic circulation. Therefore, depending on the administration and sampling sites, a series of different organs may contribute to the first pass effect.

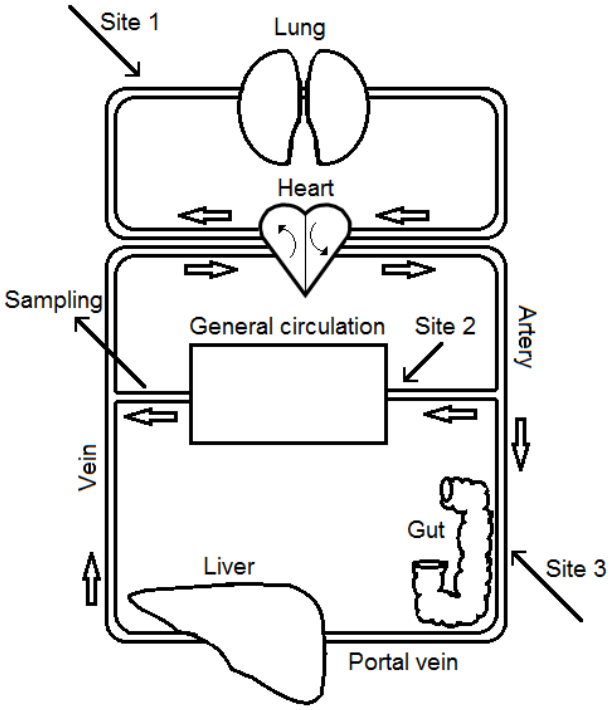

Figure 1.1. Schematic diagram of the blood circulation and three major administration sites.

Obviously the liver has a central role in ADME processes as it is quantitatively and qualitatively a very crucial site of drug metabolism. The first pass effect caused by the liver can significantly influence the plasma concentration and the efficacy of the drug. Consequently, it is required to have an insight into the liver anatomy and physiology as well as the mechanism of hepatic elimination process.

1.2.4 Liver anatomy and physiology

Liver is the largest solid organ in the body and serves a critical function in blood detoxification, drug metabolism, bile excretion for fat breakdown, blood sugar level regulation and cholesterol metabolism regulation. Liver is mostly situated in the right side of the abdominal cavity just below the diaphragm. For adults it weighs about 1600 g in average with an average volume of 1602 and 1341 ml, for males and females, respectively (Anderson et al., 2000).

Under normal conditions in human, a quarter of the cardiac output (between 1200 and 1500 ml/min) flows through the liver every minute. The liver blood is supplied by two main sources - portal vein and hepatic artery. Approximately 80% of the hepatic blood flow is supplied by the portal vein containing partially deoxygenated but nutrient-enriched blood mostly originating from the gastrointestinal tract (Garcea and Maddern, 2009). The rest of the hepatic blood flow is supplied by the hepatic artery containing fully oxygenated blood coming from the celiac trunk and descending aorta. The regulation of the hepatic blood flow is performed by controlling the hepatic arterial flow (Bonfiglio et al., 2010). The blood supply from portal vein and hepatic artery are mixed in the liver and are eventually drained into the hepatic vein leaving the liver to travel to the heart.

Figure 1.2 illustrates a schematic diagram of the cross section of the liver tissue. A microscopic view into the liver tissue reveals that the liver is composed of hexagonal cross-sectional units called acini (Fig. 1.2a). Each hexagonal unit, acinus, is mostly made hepatocytes radially arranged in thin layers from inside to the outside (Fig. 1.2b). The blood from the branches of hepatic artery and portal vein are mixed in capillaries called sinusoids through which the blood flows to the central vein. Sinusoids are vascular channels made of a thin layer of endothelial cells which are separated from the underlying hepatocytes by space of disse. As the blood flows in sinusoids, the blood is filtered by the endothelial cells so that oxygen, drug

compounds and/or toxic substances diffuse into the space of disse from which mass transfer takes place into the hepatocytes (Bonfiglio et al., 2010; Teutsch, 2005). Metabolism takes place in hepatocytes by Phase I and Phase II enzyme-mediated processes. Bile, the secreted product of hepatocytes, is excreted into a network of bile canaliculi that conduct the bile to the bile ducts from which the bile is eventually drained into the gall bladder. Eventually, bile enters the proximal duodenum upon stimulation by the consumption of a meal.

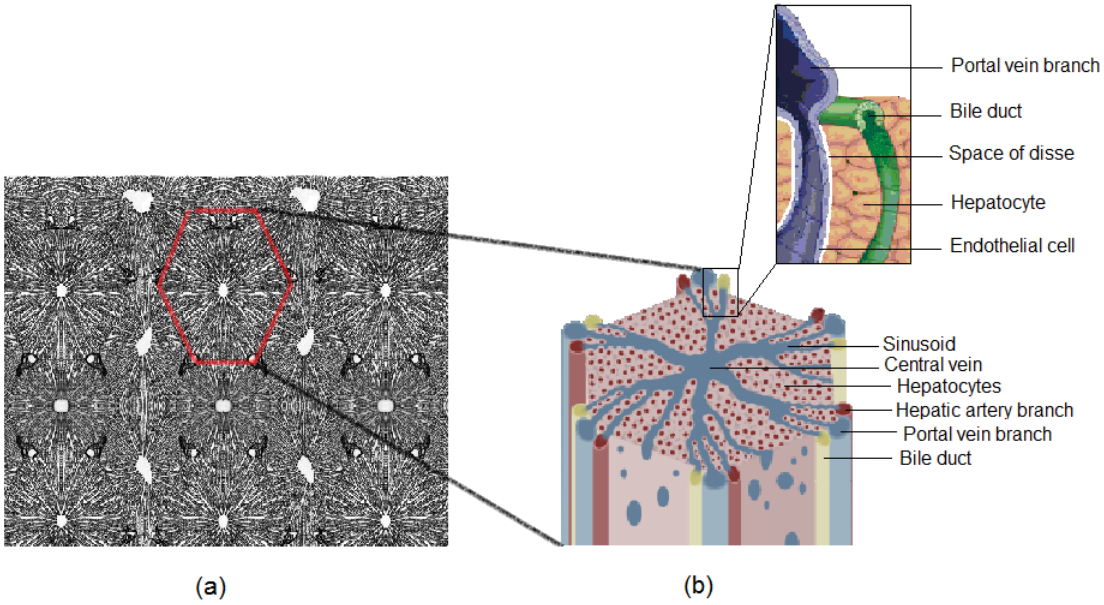

Figure 1.2. Schematic diagrams of the liver hexagonal units (a) and the microstructure of an acinus.

1.2.5 Hepatic clearance

The hepatic clearance is defined as the volume of the blood that perfuses to the liver and is cleared of drug compound per unit time. Hepatic drug elimination results from the drug metabolism and/or biliary excretion of drug in the liver. Drug metabolism is a process by which a drug is chemically changed to a metabolite with concomitant loss in pharmacological activity. Biliary excretion of a drug occurs due to the concentration gradient of unbound drug across the hepatocytes such that a higher plasma unbound drug concentration can enhance the secretary

transport of the drug in the liver. For lipophilic drugs which are not sufficiently excreted by kidneys, hepatic metabolism alters them into more water soluble compounds to be eliminated in urine and/or bile (Nebert and Russell, 2002).

For many drugs liver is the most important eliminating organ such that it urges us to identify the physiological determinants attributed to the hepatic drug uptake and removal governing the hepatic clearance. These physiological determinants are hepatic blood flow, protein binding of the drug to the blood, inherent ability of the liver for eliminating the drug (intrinsic clearance), and hepatic transport mediated uptake (Pang and Gillette, 1978). Based on how the physiological determinants influence the hepatic clearance, the drug can be high or low in hepatic ER (section 1.2.3.1) which is defined as the fraction of the drug at the liver inlet that is eliminated due to the hepatic clearance. A high or low ER drug is a drug which is highly or poorly eliminated from the blood, respectively, as it is passing though the liver. The interrelationship of the physiological determinants of hepatic clearance determines low or high hepatic ER. For example, if the inherent ability of the liver for eliminating a drug is poor, the hepatic ER of the drug remains low even if the drug presentation to the liver is high due to a high hepatic blood flow. Likewise, the hepatic ER of the drug can be still low if the drug is poorly delivered to the liver despite a high inherent ability of drug metabolism by the liver. Below the rate limiting factors influencing the hepatic clearance will be elaborated.

1.2.5.1 Intrinsic clearance

Intrinsic clearance is an indication of inherent enzyme activity in hepatocytes. Intrinsic clearance represents the maximal ability of hepatocytes to irreversibly eliminate unbound drug molecules from liver water assuming blood flow, protein binding and cell membrane

permeability are not rate limiting. Therefore, unbound intrinsic clearance can exceed the hepatic clearance in most cases.

Generally the hepatic metabolism of drugs is mediated by hepatic Phase I and Phase II enzymatic metabolism in hepatocytes. The enzymatic metabolism is performed through oxidation/reduction, hydrolysis and inactivation of functional group of the parent drug. Phase I enzymes are responsible for oxidation/reduction and hydrolysis while in Phase II pathway an endogenous molecule is conjugated to the functional group of the parent drug molecule being functionally inactivated. Another important function of Phase II enzymes is the transformation of reactive molecules that may be produced by Phase I drug metabolism (Park et al., 2005). The metabolizing P450 enzymes and some Phase II enzymes are located in the smooth endoplasmic reticulum within the hepatocytes (Ortiz de Montellano, 1995).

Hepatocellular metabolism can be influenced by drug-drug interactions and genetic polymorphisms that cause interindividual variability in hepatic drug metabolism (Tirona et al., 2003; Martinez-Jimenez et al., 2005).

In many cases, Michaelis-Menten kinetics describes the metabolism of a drug and intrinsic clearance, then, can be quantitatively determined as:

$$Cl_{int} = \frac{V_{max}}{K_M + C_u} \tag{1.8}$$

where V_{max} is the maximum enzyme activity capacity, K_M is the inverse function of affinity between the drug molecules and enzyme, and C_u is the unbound plasma drug concentration. V_{max} is a function of the enzyme concentration at the metabolizing site while the affinity term (K_M) is defined as the unbound drug concentration that leads to half of the maximum enzymatic metabolism rate. In other words, the affinity term represents the unbound drug concentration causing half of the active sites of metabolic enzymes to be saturated. Since it is impossible to

measure the unbound drug concentration at the enzyme, the estimation of K_M is made based on the unbound plasma concentration, C_u.

According to Eq. (1.8) for low unbound drug concentration, the intrinsic clearance can be assumed as a constant value of the ratio of V_{max}/K_M. However, if the affinity of a drug to the metabolic enzymes in hepatocytes is high or the concentration of drug is high, the value of K_M will be negligible compared to the unbound drug concentration resulting in a concentration dependent intrinsic clearance defined as the ratio of V_{max}/C_u. In this case, intrinsic clearance decreases as the unbound drug concentration increases. This is because the active sites of the metabolizing enzymes approach saturation when unbound concentration (C_u) exceeds K_M.

Since different enzymes can be responsible for metabolizing a particular drug, the overall metabolism process can be defined as:

$$Cl_{int} = \sum_{n=1}^{N} \frac{V_{max,n}}{K_{M,n} + C_{u,V}} \tag{1.9}$$

where n represents the n^{th} individual metabolic enzyme in hepatocytes and $C_{u,V}$ is the unbound drug concentration in the hepatic vein. Using the definition of intrinsic clearance simply given in Eq. (1.8), the hepatic metabolism rate can be defined as:

$$\vartheta = Cl_{int}\ f_{u(B)} C_p = \left(\frac{V_{max}}{K_M + C_u} \right) f_{u(B)} C_p \tag{1.10}$$

where ϑ is the rate of metabolism by the hepatocytes and C_p is the total drug concentration in plasma.

In case of good drug delivery to the liver tissue (due to sufficient blood flow) and sufficiently high unbound fraction of the drug in the blood, if the drug transfer to hepatocytes is not limited by the hepatic tissue membrane permeability, the intrinsic clearance will be the rate limiting factor of the hepatic clearance. In this case, if the intrinsic clearance is low, the metabolism of

the drug remains low despite the presence of the drug compounds. Therefore, high or low intrinsic clearance determine high or low hepatic ER of the drug.

1.2.5.2 Hepatic perfusion rate

Providing that the drug is poorly bound with blood cellular components and plasma proteins (high unbound fraction), that passive diffusion or transporters adequately mediate drug transport across cell membranes, and that the hepatocellular enzyme activity is inherently high, the drug presentation to the hepatocytes, governed by the blood flow rate, will be the deterministic factor of the hepatic clearance. Thus, the faster the drug is supplied to the liver the higher rate of drug elimination by the liver. Therefore, the perfusion rate governs the hepatic elimination rate and consequently will be the limiting factor of the hepatic clearance. In this case, higher blood flow results in higher hepatic ER (section 1.2.3.1); however, if the intrinsic clearance is low, the hepatic ER will be low despite a high blood flow. In general, if other rate limiting processes exists, the blood perfusion rate will no longer be the limiting factor of the hepatic clearance.

1.2.5.3 Drug unbound fraction

For drugs with low hepatic ER (section 1.2.5) which can be associated with low intrinsic clearance and poor transport mediated drug uptake, the unbound drug fraction becomes a rate limiting factor of hepatic clearance because with a poor transport mediated drug uptake, only unbound drugs can traverse the membranes and be metabolized. Equation (1.10) also indicates that an increase in unbound fraction has a more significant role in enhancing the metabolism rate when the intrinsic clearance is low. In contrast, if the hepatic ER of a drug is inherently high, it indicates that a significant fraction of the drug at the liver inlet is well eliminated from the blood. Therefore, even if the protein binding of the drug to the blood is high, it will not be a rate-limiting factor. As the free drug is quickly metabolised in hepatocyes, unbound drug compound

is transferred from the plasma to the tissue. It results in a departure from equilibrium in the plasma where a fraction of bound drug dissociates into unbound form. The unbound drug will be ready to traverse the membrane to be available to the enzymes. Consequently, for high ER drugs, changes in unbound fraction of a drug have no influence on the hepatic clearance. For the cases where metabolic ER is intermediate, a region of the liver may exhibit high metabolic ER while another region poses low metabolic ER due to non uniformity of the distribution of enzymes and their activity. In this case, hepatic metabolism rate can be sensitive to the unbound fraction in the regions with low ER while insensitive to the unbound fraction in the regions with high ER.

1.2.5.4 Transport mediated uptake

The hepatic metabolism rate can be limited by hepatic uptake transporters. A hepatic intrinsic clearance which includes the concepts of intrinsic clearance, influx and efflux membrane permeability can be described as (Pang et al., 1978; Yamazaki et al., 1996):

$$Cl_{in\_overall} = PS_{u,influx} \times \frac{Cl_{int}}{Cl_{int} + PS_{u,efflux}} \tag{1.11}$$

where $PS_{u,influx}$ and $PS_{u,efflux}$ are membrane permeability surface area of unbound drugs across the sinusoidal membrane for the influx and efflux processes, respectively. If the efflux is negligible compared to the intrinsic clearance, the overall intrinsic clearance is given as:

$$Cl_{in\_overall} = PS_{u,influx} \tag{1.12}$$

In this case, the hepatic uptake transporters will be rate limiting factor and subsequently determine the net intrinsic clearance and hepatic metabolism rate. It implies that even if the metabolic enzyme activity in hepatocytes is very high, the hepatic metabolism rate can be low if uptake transporters poorly perform the transport process. In contrast, if the efflux is considerably larger than the intrinsic clearance, the overall intrinsic clearance can be given as:

$$Cl_{in\_overall} = PS_{u,influx} \times \frac{Cl_{int}}{PS_{u,efflux}} \tag{1.13}$$

In this case, both influx and efflux processes affect the overall intrinsic clearance. In case of the equality of influx and efflux processes with rapid permeation of the drug across the sinusoidal membrane, the hepatic transporters have no rate limiting effect on the hepatic clearance where the net intrinsic clearance will be equal to the intrinsic clearance.

1.2.6 Bioavailability

It was discussed in Section 1.2.6, the oral administration is followed by the drug absorption from the intestinal tract into the portal vein that transports the drugs to the liver. A fraction of the drug can be potentially metabolized by the enzymes in the intestinal wall cells as well as in the blood of the portal vein. However, the majority of the drug is subject to the hepatic metabolism through the first passage across the liver. Following intestinal absorption the concentration of the drug in the portal vein is considerably high and the fraction of the drug which is subjected to hepatic elimination on the first pass through the liver can be significant. The fraction of the absorbed drug which reaches the systemic circulation is called hepatic bioavailability (F_H) and defined as:

$$F_H = 1 - \frac{C_A - C_V}{C_A} = 1 - ER \tag{1.14}$$

Equation (1.14) is based on the assumption of full perfusion of the portal vein in the liver. Equation (1.14) implies that if a drug is efficiently extracted by the liver, a small fraction of the drug may reach the systemic circulation if it is administered orally. For this type of drug, hepatic disease or drug-induced alterations, which reduce the hepatic elimination efficiency, can significantly increase the systemic bioavailability.

Oral bioavailability is defined as the fraction of the dose that reaches the systemic circulation. Oral bioavailability takes into account the unabsorbed fraction of the dose in the intestine as well as the drug loss due to the metabolism occurring in the intestine wall, portal vein and liver until the drug reaches the systemic circulation.

1.3 Physiological model for hepatic drug elimination

Physiological models are mathematical equations which can describe the mechanisms of the processes in the body based on degrees of physiological and physical simplifications and assumptions of the process. Unlike empirical models which are mainly based on the measured data, physiological/mechanistic models are developed based on the physics and the biology behind the phenomena. Physiological, chemical and physical properties and parameters are incorporated in a mechanistic model so that the model provides us a better insight into a process occurring in the body compared to kinetic and empirical models.

The liver possesses a complicated physiology and structure and has been an attractive organ for those researchers who were trying to mathematically describe hepatic functionality for prediction of hepatic drug elimination. A physiologically predictive model can allow us to analyze the influence of physiological, pharmacological and pathophysiological events on the efficiency of the hepatic drug elimination. In addition, such a model can be used for estimating PK parameters of a new drug during the drug discovery process. Several physiological models have been proposed to describe the hepatic clearance. The four well known models are well-stirred (WS), parallel tube (PT), distributed sinusoidal perfusion (DSP), and dispersion (DP) models while some other conceptual models have been proposed recently based on different sets

of assumptions and theories (Nestorov, 2007; Pang et al., 2007; Sun and pang, 2010). The principles of the models will be reviewed in this section.

1.3.1 Well-stirred model

WS model, which was inspired from the concept of well-mixed reactor for petroleum cracking in chemical reaction engineering, was first proposed by Gillette (1971) and then established by Rowland et al. (1973) and Wilkinson and Shand (1975). WS model assumes that the liver is equivalent to a perfectly mixed reaction vessel which is continuously stirred so that the fresh blood entering the liver instantaneously mixes with the blood in the liver. According to WS model the drug is homogenously distributed in the liver causing no concentration gradient across the liver. Consequently, mass balance over the liver at steady state results in (Ridgway et al., 2003):

$$C_V = \frac{Q_H C_A}{Q_H + f_{u(B)} Cl_{int}} \tag{1.15}$$

where C_V and C_A are the drug concentration at the liver inlet and outlet, respectively, and Q_H is the perfusion rate. Applying Eq. (1.15) to the definition of the hepatic clearance and bioavailability results in bioavailability and hepatic clearance mathematical expressions as:

$$F_H = \frac{1}{1 + \frac{f_{u(B)} Cl_{int}}{Q_H}} \tag{1.16}$$

$$Cl_H = \frac{Q_H f_{u(B)} Cl_{int}}{Q_H + f_{u(B)} Cl_{int}} \tag{1.17}$$

Although the WS model is based on an idealized situation which makes the model oversimplified, it is easy to use and understand and can be easily applied for rough estimation of rate limiting factors. For example, if the intrinsic clearance is much smaller than the blood flow rate, the denominator of Eq. (1.17) reduces to Q_H and Eq. (1.17) is simplified to hepatic

clearance as a function of intrinsic clearance and unbound fraction. In this case for a reasonably high unbound fraction, the enzyme activity will be rate limiting factor of the hepatic clearance. On the other hand, WS model is only valid for a steady state condition and unable to take into account the complex network of the vascular anatomy of the liver and some important physio-chemical properties such as tissue partition coefficient.

1.3.2 Parallel tube model

The concept of parallel tube (PT) model was inspired from the plug flow reactors in chemical reaction engineering. PT model became a better representation of the liver compared to WS model by assuming the sinusoids as parallel tubes with equal blood velocity and intrinsic clearance (Iwatsubo et al., 1996). PT model assumes that the drug compounds in the blood at the liver inlet enter the liver at the same time and then travel through the liver with a constant and equal velocity in parallel cylindrical tubes (Roberts and Rowland, 1986). Based on PT model, mass balance of the drug at steady state results in a nonlinear drug concentration gradient function as (Niro et al., 2003):

$$Q\frac{dC}{dz} = -\frac{f_{u(B)}Cl_{int}}{L}C \tag{1.18}$$

According to the analytical solution of Eq. (1.18), bioavailability and hepatic clearance are defined as:

$$F_H = \exp\left(-\frac{f_{u(B)}\,Cl_{int}}{Q_H}\right) \tag{1.19}$$

$$Cl_H = Q_H\left(1-\exp\left(-\frac{f_{u(B)}\,Cl_{int}}{Q_H}\right)\right) \tag{1.20}$$

Similar to WS model, the PT model can be easily used as a useful tool to assess the relationship between the hepatic clearance and unbound fraction, intrinsic clearance and the

hepatic blood flow (Wilkinson and Shand, 1975). Although PT model takes into consideration the non-uniform drug distribution in the liver and also offers a picture of the blood flow in the liver, it lacks the important transport mechanisms of diffusion, convection and dispersion for drug transport across hepatocellular membranes. In addition, both WS and PT model exclude the influence of the complex vascular network existing in the liver.

1.3.3 Distributed sinusoidal perfusion model

DSP model is the physiologically extended version of PT model. Unlike the PT model, the DSP model represents sinusoids as non-identical parallel tubes allowing the blood flow to pass through the liver while each tube contains a fraction of the hepatic blood flow (Iwatsubo et al., 1996; Bass et al., 1978). According to DSP model, the hepatic bioavailability derived for the PT model must be expressed by each individual tube with the associated fraction of the hepatic blood flow rate. Since the tubes are not identical, each tube suggests its own intrinsic clearance as the associated dispersion and flow mixing effects all of which offer the liver heterogeneity which is defined as (Bass et al., 1978):

$$\zeta^2 = \sum_{i}^{N} \left[\frac{\left(\frac{Cl_{\text{int},i}}{Cl_{\text{int}}} \right)^2}{\left(\frac{Q_{H,i}}{Q_H} \right)} \right] - 1 \tag{1.21}$$

where $Cl_{int,i}$ and $Q_{H,i}$ are intrinsic clearance and blood flow rate associated with each individual tube, i is the tube index and N is the number of tubes. Subsequently, the flow-weighted bioavailability is defined as (Bass et al., 1978):

$$F_H = \left(1 + \frac{1}{2} \zeta^2 \left(\frac{Cl_{\text{int}}}{Q_H} \right)^2 \right) \exp\left(- \frac{Cl_{\text{int}}}{Q_H} \right) \tag{1.22}$$

Although the DSP model incorporates a more realistic picture of the liver blood flow compared to PT and WS models, it is unable to characterize the distribution of residence time of the drug in the liver. In addition, similar to WS and PT models, the DSP model is valid at steady state.

1.3.4 Dispersion model

Incorporating the axial dispersion and convection of blood flow in cylindrical tubes that represent the sinusoids, the DP model has been widely accepted as a physiological based model of the liver (Roberts and Rowland, 1987). The DP model is based on the residence time distribution of the drug in the liver (Roberts and Rowland, 1986). Assuming a very small volume much smaller than the organ volume but much larger than the mean free path of molecules, the DP model was developed according to the variation of the amount of time spent on respective volumes in the organ (Roberts and Rowland, 1986). The residence time is influenced by the convection and dispersion effects of the blood flow. Axial dispersion is a major mass transport mechanism in the liver where the sinusoidal blood velocity is sufficiently high to cause a non-uniform sinusoidal blood velocity and subsequently non-uniform residence time distribution in the liver. Péclet number is a dimensionless number representing the magnitude of convection effect over the dispersion effect of a fluid flow. The inverse of Péclet number is called dispersion number (D_n) as an indication of the degree of importance of the dispersion in the drug transport in the liver. Dispersion number is defined as:

$$D_n = Pe^{-1} = \frac{D_{\parallel}^{d}}{uL} \tag{1.23}$$

Where Pe is Péclet number, $D_{\parallel}^{d}$ is the axial dispersion coefficient, and u is the linear velocity along the length of L of the cylindrical tubes. When the dispersion number goes to infinity, the mixing frequency of the blood becomes so high that the system behaves similar to WS model.

On the other hand, if the dispersion number goes to zero, the system exhibits the behaviour of PT model (Niro et al., 2003).

Assuming that the intrinsic clearance is independent of the drug concentration, Rowland and Roberts (1986) presented the variation of residence time distribution of the drug in the liver at steady state as (Roberts and Rowland, 1986):

$$Q_H D_n \frac{d^2C}{dZ^2} - Q_H \frac{dC}{dZ} - Cl_{\text{int}} C = 0 \tag{1.24}$$

where C is the plasma drug concentration normalized to the ratio of the drug dose to the volume of distribution, and Z is the dimensionless position along the liver. For the analytical solution of Eq. (1.24) the Dankwerts boundary condition was defined as (Dankwerts, 1952):

$$\begin{aligned} &C - D_n \frac{dC}{dZ} = C_{in} \quad at \quad Z = 0 \\ &\frac{dC}{dZ} = 0 \quad at \quad Z = 1 \end{aligned} \tag{1.25}$$

The analytical solution of Eq. (1.24) led to the hepatic bioavailability expression as (Dankwerts, 1952):

$$F_H = \frac{4a}{(1+a)^2 \exp\left[\frac{(a-1)}{2D_n}\right] - (1-a)^2 \exp\left[\frac{-(1+a)}{2D_n}\right]} \tag{1.26}$$

where a is defined as:

$$a = \left(1 + \frac{4D_N f_{u(B)} Cl_{\text{int}}}{Q_H}\right)^{1/2} \tag{1.27}$$

An extension to DP model has been made by incorporating a second vascular compartment to the interconnecting sinusoids (Roberts and Anissimov, 1999). Although DP model takes into account the physiological characteristics of sinusoidal blood distribution and the associated residence time of the drug in the liver, it requires a general assumption whereby no parameter

varies along the liver and also the intrinsic clearance remains independent of drug concentration. In addition, the solution of DP model is valid for a steady state approximation of unbound drug concentration in hepatocytes.

1.3.5 Interconnected-tubes model

Anissimov et al. introduced the concept of interconnected-tubes (ICT) model by modeling the hepatic elimination process using a large number of parallel and interconnected tubes interchanging the blood flow along the length of the liver (Anissimov et al., 1997). The ICT model takes into account the intermixing of the blood flow between sinusoids by a continuous and constant interchange of the drug between a set of parallel tubes at a steady state of hepatic elimination process. The ICT model includes a heterogeneity expression which characterizes the combined effects of non-uniform distributions of enzymes and flow rates between different sinusoids and also the intermixing effects of the blood flow between sinusoids (Anissimov et al., 1999). The ICT model at steady state is mathematically formulated as:

$$\mathbf{V}\frac{dC}{dx} = -\mathbf{K_e}C + \mathbf{M}C \tag{1.28}$$

where $\mathbf{V}$ is the diagonal matrix of blood velocity associated with parallel tubes, $\mathbf{K_e}$ is the diagonal matrix of the elimination rate constant, and $\mathbf{M}$ is the matrix of coefficients of exchange between tubes. According to ICT model, when the parallel tubes are poorly interconnected, the predicted drug concentration at the outlet is similar to that in DSP model and DP model for small dispersion number values.

Although ICT model conceptualizes the interconnectivity of sinusoids and intermixing of blood flow in the liver, it lacks the physiological concept and parameters involved in hepatic clearance (i.e. membrane permeability, intrinsic clearance, tissue partition coefficient) and

physio-chemical properties of the drug (i.e. unbound fraction). In addition, the elimination coefficient is assumed constant for all the tubes along the tube lengths.

1.3.6 Tanks-in-Series model

Murray et al. (1987) treated the liver as a series of adjustable number of compartments (tanks) that allow the clearance to be dependent on blood flow. The model performs as a bridge between WS and PT models. When the number of tanks approaches 1, the model results become identical to those of WS model. For large number of tanks the model exhibits the PT model (Gray and Tam, 1987). The model at steady state leads to the liver outlet drug concentration and the bioavailability, respectively, as (Gray and Tam, 1987):

$$C_N = C_{out} = C_{in}\left(1 + \frac{Cl_{int}}{NQ_H}\right)^{-N} \tag{1.29}$$

$$F_H = \left(1 + \frac{Cl_{int}}{NQ_H}\right)^{-N} \tag{1.30}$$

where N is the number of tanks. For the non-linear elimination kinetics, the model is reformed as:

$$C_i = \frac{a}{2} + \left(\frac{a^2}{4} + K_M C_{i-1}\right)^{1/2}$$
$$a = C_{i-1} - K_M - \frac{V_{\max}}{Q_H N} \tag{1.31}$$

where K_m and V_{max} are the affinity and maximum metabolism rate capacity terms.

Like WS and PT model, the tank-in-series model is unable to physiologically describe the effect of dispersion and convection and intermixing effects of blood flow in the liver. However, the key advantage of such compartmental models is the simplicity of the equations. Also,

compartmental models can be easily reformulated for more complex situations such as heterogeneous enzyme distribution in the liver.

1.3.7 Recent model orientations

In recent years, researchers have focused on extending the models so that the heterogeneity in blood flow, enzymes, and transporters are included. Liu and Pang (2006) adopted an integrated approach to predict hepatic drug clearance in such a way to include the heterogeneity in enzymes and transporters. Fan et al. (2010) utilized physiologically based pharmacokinetic intestinal and liver models to predict the contributions of enzymes and transporters on intestinal availability and the hepatic availability of the drug. They included the impact of the influx and efflux transport processes to evaluate the intestine and the liver clearances (Fan et al., 2010).

The use of the physiological models becomes difficult when unsteady state and nonlinear hepatic pharmacokinetics and enzyme heterogeneity exist. Hisaka and Sugiyama (1998) solved the fundamental equation of DM at nonlinear and unsteady state hepatic elimination of substances using explicit finite difference method which is less accurate than the implicit method. They also incorporated their method into a nonlinear least-squares fitting algorithm to estimate PK parameters. Their numerical model was a resemblance of a series of *m* compartments corresponding to the free or bound drug in the vascular space, blood cells, or Disse space, or in the cells at various radial distances from the vasculature; however, the model was unable to include the equilibrium condition, represented by tissue partition coefficient, between the tissue cells and the blood. Also the model was lacking the structural properties of the liver tissue (i.e. porosity, tortuosity).

A promising approach that has emerged recently to assist scientists to analyze biological systems is the porous media approach. Since biological systems are made of a dispersed phase (i.e. cells) in a continuous phase of a fluid (i.e. blood or extracellular fluid), they can be treated

as porous media. In the same way, porous media principles can be applied to human tissues/organs where dispersed cells are separated by connective voids that allow the blood/extracellular matrix flow though the tissue. Porous media approach has been successfully applied to some biosystems including cartilage tissue engineered scaffold development (Izadifar et al., 2011), radio frequency enhanced extraction of anti-cancer compounds from a biological system (Izadifar and Baik, 2010), and thermotherapy and human thermoregulation system (Sherar et al., 2001; Sanyal and Maji, 2001). The liver is a highly perfused tissue which can be appropriately treated as a porous medium. Charles et al. (1989) introduced a three dimensional finite element model for the fluid flow and mass transfer in the liver based on the principles of porous media. Assuming a Reynolds number smaller than 1, they adopted the principles of porous media where the blood flow in the liver was a creeping flow described by Darcy's law. They developed the momentum equation according to the hydraulic permeability of the tissue. For the mass transfer equation, they assumed the Peclet number to be greater than 1 whereby the dispersion could be neglected due to the dominant convection. The mass transfer governing equation was unable to describe the hepatocellular drug metabolism which can be linear or nonlinear. In addition, the model was unable to include the tissue-blood equilibrium of the drug species but the drug transfer from the blood to the cells was described based on the cell membrane permeability. The lack of information of tissue partition coefficient, the axial dispersion and hepatocellular metabolism in the model were significant downsides of the proposed model.

The following section brings a brief overview of some important porous media concepts to the readers. It will be followed by introducing the objective of this research which is to apply porous media concepts to mathematically describe hepatic drug elimination process.

1.4 Porous media concepts and applications in biomedical engineering

Porous medium is defined as a solid matrix with interconnected voids filled with a fluid, liquid or gas or both. The solid matrix can be particles of the soil, the polymer matrix of a tissue engineering scaffold, a packed bed of fertilizer particles, or a vascularised tissue. A porous medium is generally characterized by porosity, length scales, tortuosity and permeability. Modeling of transport phenomena of porous media made significant progress recently and the models have been used for different applications in engineering and science. In this section the concepts and biological applications of porous media are reviewed and discussed.

1.4.1 Representative elementary volume (REV)

A porous medium is a solid matrix consisting of a solid phase and spaces among solid particles which can be filled with a fluid, liquid or gas. The range of pore size of porous media can vary from molecular size (nm) to centimetre. When a solid matrix cannot be described within a pore size, a REV with a characteristic length of l and volume of V_l is defined to represent the structure of the solid matrix. REV is defined as the smallest differential volume of a porous medium that results in statistically meaningful average properties of the porous medium (Darcy, 1856). Figure 1.3 schematically and graphically depicts the concept of a REV. As it can be seen, a very small volume located in the pore of the porous medium (Fig. 1.3a) results in the fluid volumetric fraction of 1 as indicated in Fig. 1.3b. As the size of the volume increases, more solid fraction is included in the volume causing the fluid volumetric fraction to decrease. As it is shown in Fig. 1.3 b, the variation of the fluid volumetric fraction fluctuates with the size of the volume; however, it becomes insensitive to any increase in the size of the volume when the volume of V_l is sufficiently large. The volume of V_l, which is called REV, is the smallest volume the property of which can represent the property of the porous medium.

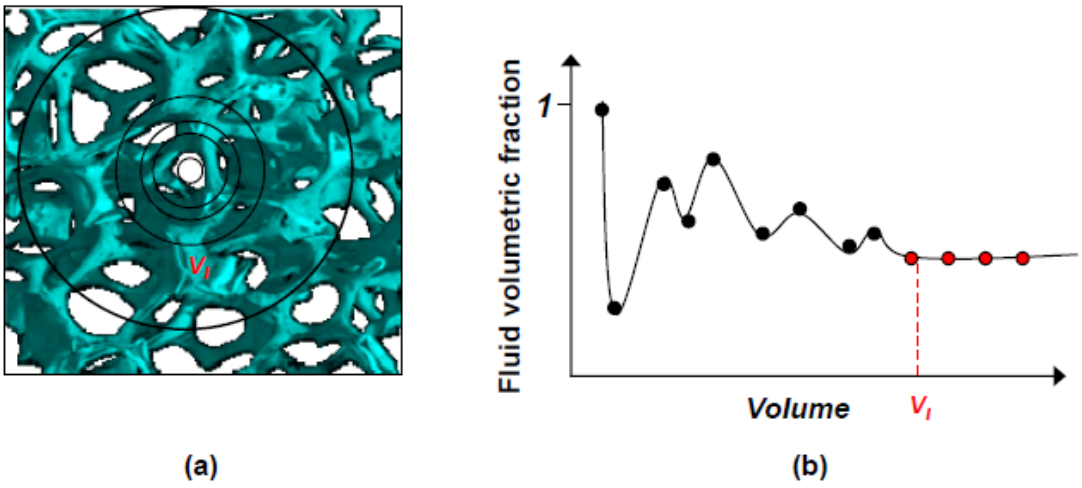

Figure 1.3. Schematic diagram of representative elementary volume and the variation of the medium property with the size of representative elementary volume.

1.4.2 Local volume averaging method (LVA)

Averaging properties of the medium over REV is called local volume average properties of the medium. If a property of one of the phases of the REV is averaged over the volume of the phase, it is called intrinsic phase averaged property. Averaging the governing equations of mass, heat and momentum transfer over the REV with the application of local volume average properties is called the LVA method to describe transport phenomena in porous media.

1.4.3 Length scales in porous media and LVA validity condition

In order to apply the concept of LVA method to mathematical modeling of transport phenomena in a porous medium, the length scales of the medium must satisfy the validity condition of LVA method. Figure 1.4 illustrates the characteristic lengths of a typical porous medium. The characteristic lengths of a porous medium are: the linear dimension of the porous medium system (L), the REV characteristic length (l), the pore size (d_p), and Brinkman screening distance ($K^{1/2}$), which is an indication of the boundary layer thickness of the fluid flowing in pores of the medium.

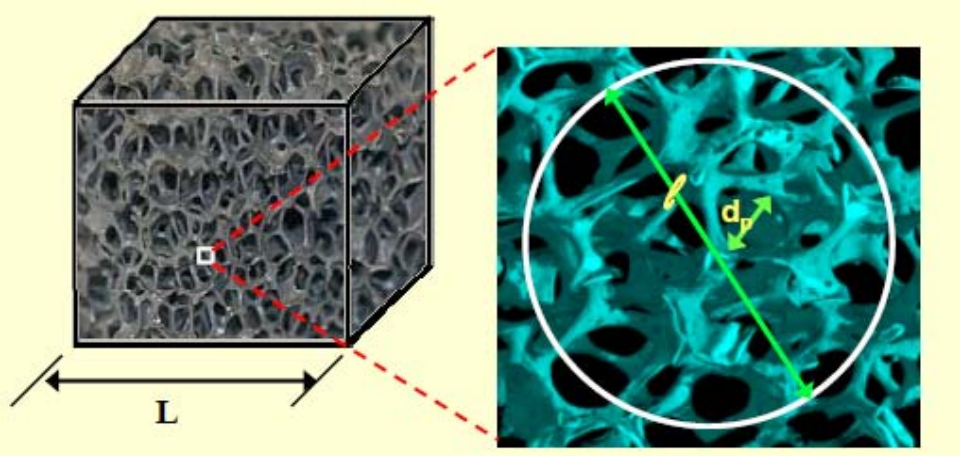

Figure 1.4. Schematic diagram of a porous medium and the associated length scales.

The validity condition of LVA method is:

$$K^{1/2} << dp < l < L \tag{1.32}$$

where K is the permeability of the porous medium. Permeability is an important property and a measure of the flow conductivity in the porous medium. According to Darcy law, the fluid velocity is linearly related to the pressure gradient across the porous medium with a proportionality constant of the ratio of permeability to the fluid viscosity (Darcy, 1856). A porous medium is also characterized by tortuosity which is defined as the ratio of the length of the tortuous path to the straight length between both ends of the porous medium. A plain medium (a non-porous medium) possesses a tortuosity of 1 while for a porous medium the tortuosity is greater than 1. Tortuosity has a great impact on the molecular diffusion and heat conduction across a porous medium.

1.4.4 Application of LVA method to biological systems

LVA method has been used for developing mechanistic models of numerous biological systems. Izadifar et al. (2011) applied LVA method to develop a mathematical model for mass transfer of nutrients and chondrocyte proliferation in a cylindrical cartilage scaffold. These

researchers developed two sets of partial differential equations for glucose transfer across and cell proliferation porous scaffold based on the LVA method. The governing equations were simultaneously solved using numerical methods to analyze and predict the required time for cell seeding in biomanufacturing fabrication and superficial cell seeding methods (Izadifar et al., 2011). Izadifar and Baik (2010) developed a dynamic mathematical model of heat transfer to describe the radio frequency enhanced extraction of podophyllotoxin from a porous biological packed bed based on LVA method. Their model had very good agreement with the experimental data indicating that the LVA based model could be successfully used for optimizing the bioprocess. Sanyal and Maji (2001) treated three layers of the skin and subcutaneous region as porous media in an attempt to find the analytical and numerical solution of bioheat transfer equation to describe the human thermoregulation system under variable physiological parameters and atmospheric conditions. Nicholson (2001) developed a mass transfer model based on porous media principles to describe glucose and oxygen transfer from the vascular system to the brain cells as well as the drug delivery to the brain. He characterized the brain tissue and diffusion-generated concentration distribution by the porosity and tortuosity of the brain. His model revealed that an increase in the tortuosity and a decrease in the porosity have significant effects in reducing the effective mass diffusivity of molecules in the brain (Nicholson, 2001). Lei et al. (1998) developed a complex model for mass transfer phenomenon in transvascular exchange and extravascular transport of fluid and macromolecules for a spherical tumor. They treated both tissue and the tumor as porous media with a Darcy velocity of the blood flow while the interstitial fluid was assumed to obey Starling law. Their model proved to have good agreement with observations.

The liver is a highly perfused organ with a porous structure of hexagonal units called acini. The blood flow conductivity of the liver tissue is determined by the interconnected sinusoids in the liver. Although hepatic drug elimination has been mathematically described by different physiological models, as discussed in Section 1.3, the mass transfer phenomena in the liver has not been described from a porous media viewpoint using LVA method. The inherently porous structure of the liver allows us to describe the hepatic drug elimination process based on a porous media approach.

1.5 Research objective

The main objective of this study was to develop and validate a porous media model based on local volume averaging (LVA) method for describing the time dependent drug concentration gradient across the liver as well as drug hepatic elimination rate, hepatic clearance and hepatic bioavailability. LVA method will integrate the properties and mass transfer equations as well as the hepatocellular metabolism characteristics over the REV of the liver tissue. The main difference between LVA method and the multi-dimensional method proposed by Charles et al. (1989) is that LVA method will include the axial/radial dispersion, local volume equilibrium between tissue and blood, and time-space dependent hepatocellular metabolism in the porous media model while the model proposed by Charles et al. (1989) excluded these important events. In Chapter 2, the theoretical background of the porous media approach will be explored. The liver structure will be characterized based on four characteristic length scales and LVA validity condition will be evaluated. Then, the mathematical modeling procedure will be presented from fundamental beginnings where the mechanisms of mass transport are elaborated in a differential element of the liver tissue. The governing partial differential equation of drug transport and

nonlinear/linear drug elimination processes will be derived followed by the details of the numerical solution of the model. The stability and consistency of the numerical solution will be examined and simulation results will be compared to experimental data as well as the predicted values from other models. At the end of Chapter 2, it will be shown how the proposed model can be applied to perform the sensitivity analyses of hepatic drug elimination as well as the drug distribution in the liver with respect to different physiological conditions.

This study will assess two major hypotheses. The first hypothesis is that characteristic length scales of the liver tissue including sinusoidal diameter (pore size), acinus diameter and tissue equivalent length scale can satisfy LVA validity condition such that LVA method can be applied for modeling the hepatic drug elimination process. The second hypothesis is that the hepatic drug elimination process can be successfully described by a mechanistic model which is based on the porous media approach of LVA. The validity of the hypothesis will be assessed using observations reported by other researchers for eight different drugs with a wide range of intrinsic clearance and unbound fraction.

References:

Anderson V., J. Sonne, S. Sletting and A. Prip. 2000. Volume of the liver in patients correlates to body weight and alcohol consumption. *Alcohol & Alcoholism* 35: 531-532.

Anissimov Y.G., A.J. Bracken and M.S. Roberts. 1997. Interconnected-tubes model of hepatic elimination. *J. Theor. Biol*. 188:89-101.

Anissimov Y.G., A.J. Bracken and M.S. Roberts. 1999. Interconnected-tubes model of hepatic elimination: steady state consideration. *J. Theor. Biol* 199:435-447.

Bass L., P. Robinson and A.J. Bracken. 1978. Hepatic elimination of flowing substrates: the distributed model. *J. Theor. Biol* 72:161-184.

Benet L.Z. 2010. Clearance (née Rowland) concept: a downdate and an update. *J. Pharmacokinet. Pharmacodyn.* 37: 529-539.

Bonfiglio A., K. Leungchavaphongse, R. Repetto and J.H. Siggers. 2010. Mathematical Modeling of the Circulation in the Liver Lobule. *J. Biomech. Eng.* 132: 1-10.

Charles Y., C. Lee, B. Rubinsky. 1989. A multi-dimensional model of momentum and mass transferrin the liver. *Int. J. Heat Mass Transfer* 32: 2421-2434.

Dankwerts P.V. 1952. Continuous flow systems-distribution of residence times. *Chem. Eng. Sci* 2:1-18.

Darcy H.R.P.G. 1856. Les Fontaines Publiques de la volle de Dijon, Vector Dalmont, Paris.

Nicholson C. 2001. Diffusion and related transport mechanism in brain tissue. *Rep. Prog. Phys.* 64:815-884.

Fan J., S. Chen, E.C. Chow and K.S. Pang. 2010. PBPK modeling of intestinal and liver enzymes and transporters in drug absorption and sequential metabolism. *Curr. Drug Metab.* 11:743-761.

Garcea G. and G. J. Maddern. 2009. Liver failure after major hepatic resection. *J. Hepatobiliary Pancreat. Surg.* 16: 145-155.

Gillette J.R. 1971. Factors affecting drug metabolism. *Ann. NY Acad. Sci.* 179: 43-66.

Gray M.R. and Y.K. Tam. 1987. The series-compartment model for hepatic elimination. *Drug Metab. Dispos* 15:27-31.

Hisaka A, Y. Sugiyama. 1998. Analysis of nonlinear and nonsteady state hepatic extraction with the dispersion model using the finite difference method. *J. Pharmacokinet. Biopharm.* 26: 495-519.

Iwatsubo T., N. Hirota, T. Ooie, H. Suzuki and Y. Sugiyama. 1996. Prediction of in vivo drug disposition from in vitro dara based on physiological pharmacokinetics, *Biopharm. Drug Dispos.* 17:273-310.

Izadifar M. and O.D. Baik. 2010. Heat transfer modeling of radio frequency assisted packed bed extraction of an anticancer agent (podophyllotoxin). *Biochem. Eng. J*. 50:37-46.

Izadifar M., O.D. Baik, D. Chen. 2011. Simulation of cell proliferation in a cartilage scaffold during in vitro cell cultivation: bio-manufacturing versus superficial cell seeding methods, *18th Annual Life and Health Sciences Research day*, Saskatoon, SK, Canada, March 11.

Kaviany M. 1995. Principles of Heat Transfer in Porous Media, second ed., Springer, New York.

Lei X.X., W.Y. Wu, G.B. Wen and J.G. Chen. 1998. Mass transport in solid tumors (I)-fluid dynamics. *Appl. Math. Mech. Eng* 19:1025-1032.

Levitt D.G. 2010. Quantitative relationship between the octanol/water partition coefficient and the diffusion limitation of the exchange between adipose and blood. *BMC Clinical Pharmacology* 10:1-13.

Liu L. and K.S. Pang. 2006. An integrated approach to model hepatic drug clearance. *European J. Pharm. Sci.* 29:215-230.

Martinez-Jimenez C.P., M.J. Gomez-Lechon, J.V. Castell and et al. 2005. Transcriptional regulation of the human hepatic CYP3A4. *Mol. Pharmacol.* 67: 2088-2101.

Nebert D.W. and D.W. Russell. 2002. Clinical importance of the cytochromes P450. *Lancet* 360: 1155-1162.

Nestorov I. 2007. Whole-body physiologically based pharmacokinetic models. *Expert Opin. Drug Met.*, 3:235-249.

Niro R., J.P. Byers, R.L. Fournier and K. Bachmann. 2003. Application of a convective-dispersion model to predict in vivo hepatic clearance from in vivo measurements utilizing cryopreserved human hepatocytes. *Curr. Drug Metab.* 4:357-369.

Ortiz de Montellano P.R. 1995. Cytochrome P-450: Structure, Mechanism and Biochemistry, 2nd ed. New York, Plenum Press.

Pang, K.S. and J.R.Gillette.1978. Kinetics of metabolite formation and elimination in the perfused rat liver preparation: differences between the elimination of preformed acetaminophen and acetaminophen formed from phenacetin. *J. Pharmacol. Exp. Ther.* 207:178-194.

Pang K.S., M. Weiss and P. Macheras. 2007. Advanced Pharmacokinetic Models Based on Organ Clearance, Circulatory, and Fractal Concepts. *AAPS J.* 9: E268-E283.

Park B.K., N.R. Kitteringham, J.L. Maggs and et al. 2005. The role of metabolic activation in drug-induced hepatotoxicity. *Annu. Rev. Pharmacol. Toxicol.* 45:177-202.

Ridgway D., J.A. Tuszynski and Y.K. Tam. 2003. Reassessing models of hepatic extraction. *J. Biol. Phys.* 29:1-21.

Roberts M.S. and M. Rowland. 1986. A dispersion model of hepatic elimination: 1. Formulation of the model and bolus considerations, *J. Pharmacokinet. Biopharm.* 14: 227-261.

Roberts M.S. and M. Rowland. 1987. A dispersion model of hepatic elimination, based on the residence time distribution of blood elements within the liver. *J. Pharmacokinet. Biopharm.* 14:289-307.

Roberts M.S. and Y.G. Anissimov. 1999. Distribution Kinetics with the Extended. Convection-Dispersion Model. *J. Pharmacokinet. Pharmacodyn.* 27:343-382.

Rowland M, L.Z. Benet and G.G. Graham. 1973. Clearance concepts in pharmacokinetics. *J. Pharmacokinet. Biopharm.* 1:123-135.

Sanyal D.C. and N.K. Maji. 2001. Thermoregulation through skin under variable atmospheric and physiological conditions. *J. Theor. Biol.* 208:451-456.

Sherar M.D., A.S. Gladman, S.R.H. Davidson, J. Trachtenberg and M.R. Gertner. 2001. Helical antenna arrays for interstitial microwave thermal therapy for prostate cancer: tissue phantom testing and simulations for treatment. *Phys. Med. Biol.* 46:1905-1918.

Shitara, Y., H. Sato and Y. Sugiyama. 2005. Evaluation of drug–drug interaction in the hepatobiliary and renal transport of drugs. *Annu. Rev. Pharmacol. Toxicol.* 45:689-723.

Sun H., K. S. Pang. 2010. Physiological modeling to understand the impact of enzymes and transporters on drug and metabolite data and bioavailability estimates. *Pharmaceut. Res.* 27:1237–1254.

Teutsch H. 2005. The modular microarchitecture of human liver. Hepatology Philadelphia, PA.

Tirona R.G., W. Lee, B.F. Leake and et al. 2003. The orphan nuclear receptor HNF4α determines PXR- and CAR-mediated xenobiotic induction of CYP3A4. *Nature Med.* 9:220-224.

Wilkinson G.R., and D.G. Shand. 1975. Commentary: a physiological approach to hepatic drug clearance. *Clin. Pharmacol. Ther.* 18:377-390.

Yamazaki M., H. Suzuki and Y. Sugiyama. 1996a. Recent advances in carrier-mediated hepatic uptake and biliary excretion of xenobiotics. *Pharm. Res.* 13:497-513.

Yanni S. and D.R. Thakker. 2007. Prodrugs: Absorption, Distribution, Metabolism, Extraction (ADME) Issues, Springer, New York.

CHAPTER 2

A POROUS MEDIA APPROACH FOR MECHANISTIC MODELING OF DRUG ELIMINATION BY THE LIVER

M. Izadifar[a], O.D. Baik[b], J. Alcorn[c]

[a] *Division of Biomedical Engineering, College of Engineering, University of Saskatchewan, Saskatoon, SK, Canada*
[b] *Department of Chemical and Biological Engineering, College of Engineering, University of Saskatchewan, Saskatoon, SK, Canada*
[c] *Division of Pharmacy, College of Pharmacy and Nutrition, University of Saskatchewan, Saskatoon, SK, Canada*

Abstract

Applying local volume averaging method and local equilibrium to the liver as a porous medium, a governing equation taking into account liver porosity, tortuosity, permeability, unbound drug fraction and hepatic tissue partition coefficient, drug-plasma diffusivity, axial/radial dispersion and hepatocellular metabolism parameters was developed. The governing equation was numerically solved to predict changes in dug concentration with time and position across the liver and the hepatic clearance and bioavailability following an intravenous drug administration. The predicted values of hepatic clearance and bioavailability had good agreement with the reported observations for high and low clearance drugs. As well, the model was able to successfully predict an unsteady state of hepatic drug elimination with concentration dependent intrinsic clearance. When statistically compared to the well-stirred, parallel tube and dispersion models the proposed model suggested a smaller mean squared prediction error and very good

agreement to reported observations for eight drugs. A sensitivity analysis revealed that an increase in liver porosity results in a slight decrease in the drug concentration gradient across the liver while higher tissue partition coefficient values increase the concentration gradient. The model also suggested that the bioavailability was sensitive to the interaction between unbound fraction and intrinsic clearance. This study indicates that the liver and the hepatic drug elimination can be successfully explored from a porous media viewpoint and may provide better mechanistic predictions to drug elimination processes by the liver.

2.1 Introduction

The liver plays a very important role in the elimination of drugs, toxic substances, and harmful biochemical products produced by the body. The liver receives nutrient rich but poorly oxygenated blood from the intestines via the portal vein and oxygenated blood from the hepatic artery accounting for 75% and 25% of total blood supply, respectively. Both blood supplies perfuse to each hexagonal functional unit called acinus in which portal and arterial blood are mixed in the smallest acini vessels called sinusoids and in which mass exchange takes place between blood and hepatocytes.

The liver's essential role in the maintenance of homeostasis as well as drug and toxin elimination in the body demands a detailed understanding of liver function. Mechanistic models that effectively describe liver function can play an important role in understanding and predicting drug concentration and hepatic metabolic performance. Different physiological models have been developed for the liver based on different degrees of simplifications and assumptions. The well-stirred (WS) model and the parallel-tube (PT) model are the two most commonly used models describing drug elimination by the liver (Pang and Rowland, 1977). These models are

based on idealized situations of blood flow and drug distribution in the liver with an implicit assumption that the partition ratio of free drug between sinusoidal blood and hepatocytes is constant. In the well-stirred model, the drug is assumed to be instantaneously and homogeneously mixed with the blood in the liver resulting in very uniform drug concentration across the liver. Bass et al. (1977) and Forker and Luxon (1977) developed a distributed model representing blood flow in parallel tubes where each tube transports a volumetric fraction of total blood flow as determined by a distribution function. Roberts and Rowland (1986) developed a physiological-based dispersion (DP) model which was based on the residence time distribution of the drug in the liver where the distribution of residence times depended upon the axial dispersion. The analytical solution of the DP model requires a general assumption whereby no parameter varies along the length of sinusoids and intrinsic clearance due to metabolic enzyme activity or transporter function are independent of drug concentration. In addition, it assumes a steady state approximation of unbound drug concentration in hepatocytes. Although the DP model takes into account hepatocellular permeability of drugs, it fails to consider the hepatic tissue partition coefficient and tissue structural characteristics such as porosity and tortuosity. Hisaka and Sugiyama (1998) solved the fundamental equation of DM at nonlinear and unsteady state hepatic elimination of substances using explicit finite difference method which is less accurate than the implicit method. They also incorporated their method into a nonlinear least-squares fitting algorithm to estimate PK parameters. Their numerical model was a resemblance of a series of *m* compartments corresponding to the free or bound drug in the vascular space, blood cells, or Disse space, or in the cells at various radial distances from the vasculature; however, the model was unable to include the instantaneous equilibrium conditions (i.e. tissue partition coefficient) between the tissue cells and the blood. In addition, the structural properties

of the liver tissue (i.e. porosity, tortuosity) were not included in the model. Charles et al. (1989) introduced a three dimensional finite element model for the fluid flow and mass transfer in the liver based on the principles of porous media. Assuming a Reynolds number smaller than 1, they adopted the principles of porous media where the blood flow in the liver was a creeping flow described by Darcy's law. They developed the momentum equation according to the hydraulic permeability of the tissue. For the mass transfer equation, they assumed the Peclet number to be greater than 1 where the dispersion could be neglected due to the dominant convection. The mass transfer governing equation was unable to describe the hepatocellular drug metabolism which can be linear or nonlinear. In addition, the model was unable to include the tissue-blood equilibrium of the drug species but the drug transfer from the blood to the cells was described based on the cell membrane permeability. The lack of information of tissue partition coefficient, the axial dispersion and hepatocellular metabolism in the model were significant downsides of the proposed model.

The main objective of this study is to develop and validate a porous media model based on local volume averaging (LVA) method for describing the time dependent drug concentration gradient across the liver as well as drug hepatic elimination rate, hepatic clearance and bioavailability. Unlike the DP model, the proposed model takes into account an unsteady state drug concentration in the liver as well as concentration dependent hepatocellular metabolism which varies with time and position along the liver. In addition, unlike WS, PT and DP models, the proposed mechanistic model includes structural characteristics of the liver (i.e. porosity and tortuosity). Finally, the model considers transport properties such as axial/radial dispersion, molecular diffusion, and hepatic tissue partition coefficient. The model was used for prediction of hepatic clearance and bioavailability as well as the drug concentration gradient across the liver

with time. Also, a sensitivity analysis was performed using the model to investigate the influence of different parameters on drug distribution in the liver and hepatic elimination. The flexibility of the model was demonstrated through its coupling with an absorption model to simulate the dynamic changes in drug distribution in the liver associated with the gastrointestinal absorption process.

2.2 Theory

2.2.1 Local Volume Averaging (LVA) method

A porous medium is a solid matrix consisting of a solid phase and spaces which can be filled with a fluid. As a highly perfused tissue the liver can be treated as a porous medium consisting of sinusoidal spaces filled with blood and a matrix of hepatocytes. In porous media when a solid matrix cannot be described within pore size, a representative elementary volume (REV) with a characteristic length of l and volume of V_l is defined to represent the structure of the solid matrix. A REV is defined as the smallest differential volume resulting in statistically meaningful average properties of the porous medium. As shown in Figure 2.1, the liver tissue is composed of repeating hexagonal units of acini. Each hexagonal unit, or acinus, consists of hepatocytes lining blood-filled sinusoids of diameter, d_p. Blood from branches of the portal vein and hepatic artery is mixed and flows through the sinusoids to subsequently drain into the central vein. Substances (e.g. oxygen, drugs) are transferred from the blood to the hepatocytes during flow through the sinusoids. For the liver an acinus can be considered as a REV where averaging a property over the volume of an acinus (V_l) is called local volume averaged property defined as:

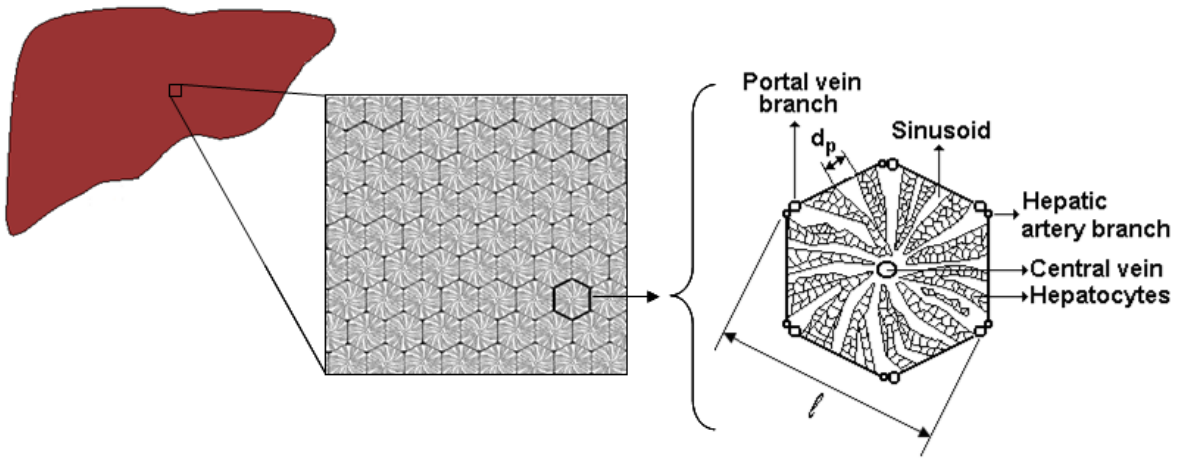

Figure 2.1. Schematic diagram of the liver microstructure with the associated length scales.

$$\langle \varphi \rangle = \frac{1}{V_l} \int_{V_l} \varphi \, dV \tag{2.1}$$

where φ is the property of interest and $\langle \varphi \rangle$ is the local volume averaged property.

The method that uses local volume averaged transport governing equations and properties over the REV is called local volume averaging (LVA) method. In order to apply LVA method, the validity of LVA must be verified by the following condition as:

$$k_{phys}^{1/2} << d_p < l << L \tag{2.2}$$

where k_{phys} is the sinusoidal based permeability (m^2), d_p is the average sinusoidal diameter (m), l is the length scale of REV (m), and L is the equivalent length of the liver tissue (m). Since a liver approximately consists of one million acinii (Jones and Spring-Mills, 1988), the REV characteristic length of a normal liver with a volume of 1223 ± 217 cm^3 will be approximately 600 μm (Zhou et al., 2007). Considering that the sinusoidal based permeability is 3.3×10^{-13} m^2 (Smye et al., 2007) and the sinusoid diameter of the liver tissue with a length of ~20 cm is as small as a few cells (i.e. <60 μm), the validity condition of LVA is satisfied as $5.7\times10^{-7}<<6\times10^{-5}<6\times10^{-4}<<2\times10^{-1}$.

2.2.2 Mathematical Modeling

The geometry of the liver was simplified so that a slab with the same thickness and volume as the liver could represent the liver tissue (Figure 2.2). Having an average volume and thickness of the liver, the length of the representative slab was calculated as the equivalent length of the liver. Figure 2.2a illustrates the liver representative slab with an equivalent length of L where the blood enters the slab through the portal vein and hepatic artery and leaves the tissue through the hepatic vein. Figure 2.2b shows the schematic diagram of a porous differential element with a length of Δx. Transport of drug into/out of the porous differential element is due to the molecular diffusion, axial/radial dispersion, and advection.

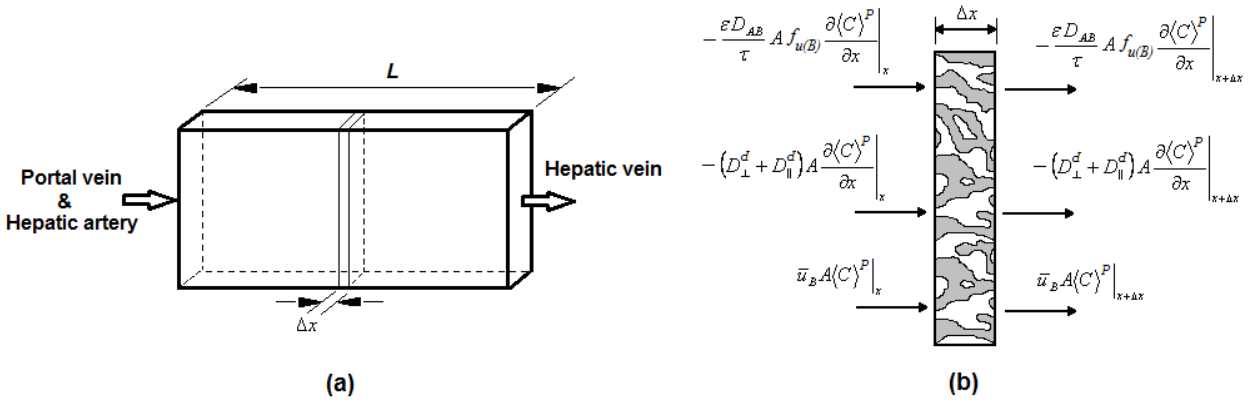

Figure 2.2. Schematic diagram of the simplified geometry (a) and the porous differential element (b) of the liver.

As the blood flows through the sinusoids (pores of the element) with a Darcy velocity, the unbound drug in plasma is assumed to be locally in equilibrium with the hepatocytes within which the drug undergoes hepatocellular metabolism at a metabolism rate described by definition as:

$$\hat{m}_{met} = Cl_{int\_invivo}\, f_{u(B)} \langle C \rangle^{P} \tag{2.3}$$

where $\hat{m}_{met}$ is the hepatocellular metabolism rate normalized by liver tissue volume ($mgs^{-1}ml^{-1}$),

$f_{u(B)}$ is the unbound fraction of the drug in the blood, $Cl_{int\text{-}in\ vivo}$ is the average value of *in vivo* hepatic intrinsic clearance (s^{-1}), and $\langle C \rangle^P$ is the local volume averaged drug concentration in plasma ($mgml^{-1}$). In addition to Eq. (2.3), the concentration dependent hepatocellular metabolism can be described by Michaelis–Menten equation as:

$$\hat{m}_{met} = \frac{V_{\max} f_{u(B)} \langle C \rangle^P}{K_M + f_{u(B)} \langle C \rangle^P} \tag{2.4}$$

where V_{max} and K_M are the maximum metabolism rate capacity ($mgs^{-1}ml^{-1}$) and affinity term ($mgml^{-1}$), respectively. Applying a transient mass balance over the differential element with a thickness of Δx results in:

$$\begin{aligned} &\left(-\frac{\varepsilon D_{AB}}{\tau} A f_{u(B)} \frac{\partial \langle C \rangle^P}{\partial x} \right)\Bigg|_x - \left(-\frac{\varepsilon D_{AB}}{\tau} A f_{u(B)} \frac{\partial \langle C \rangle^P}{\partial x} \right)\Bigg|_{x+\Delta x} + \bar{u}_B A \langle C \rangle^P \Big|_x - \bar{u}_B A \langle C \rangle^P \Big|_{x+\Delta x} - \dot{m}_{met} \\ &+ \left(-\left(D_{\perp}^d + D_{\parallel}^d \right) A \frac{\partial \langle C \rangle^P}{\partial x} \right)\Bigg|_x - \left(-\left(D_{\perp}^d + D_{\parallel}^d \right) A \frac{\partial \langle C \rangle^P}{\partial x} \right)\Bigg|_{x+\Delta x} = \frac{\Delta \left((1-\varepsilon) A \Delta x K^* f_{u(B)} \langle C \rangle^P + \varepsilon A \Delta x \langle C \rangle^P \right)}{\Delta t} \end{aligned} \tag{2.5}$$

where D_{AB} is the molecular diffusion of the unbound drug in the plasma (m^2s^{-1}), ε is the sinusoidal based porosity, τ is the sinusoidal based tortuosity, $f_{u(B)}$ is the unbound fraction of the drug in the blood, A is the cross sectional area perpendicular to the hepatic blood flow into the liver tissue representative slab (m^2), x is the position of the drug compound in the liver (m), $\dot{m}_{met}$ is the hepatocellular metabolism rate (mgs^{-1}), K^* is the liver tissue partition coefficient, t is time (s), $D_{\perp}^d$ and $D_{\parallel}^d$ are axial and radial dispersion coefficients (m^2s^{-1}), respectively, and $\bar{u}_B$ is the blood Darcy velocity (ms^{-1}) which can be given as:

$$\bar{u}_B = \frac{Q_h}{A} \tag{2.6}$$

where Q_h is the hepatic perfusion rate (mls^{-1}). In addition to Eq. (2.6), having the sinusoidal

permeability of the liver tissue and the blood pressure drop across the liver, the blood Darcy velocity can be obtained as:

$$\bar{u}_B = -\frac{k_{phys}}{\mu}\frac{\Delta P}{L} \tag{2.7}$$

where $\Delta P/L$ is the linear blood pressure gradient (Pas.m^{-1}) across the liver and μ is the blood viscosity (Pas.s).

The partial differential governing equation of drug transfer, Eq. (2.8), then, is derived by substitution of the metabolism term by Eq. (2.3) and division of Eq. (2.5) by the volume of the differential element followed by simplification of the equation and letting Δx and Δt go to zero:

$$\left(D_{\perp} + D_{\parallel} + \frac{D_{AB}\,\varepsilon\, f_{u(B)}}{\tau}\right)\frac{\partial^2 \langle C\rangle^P}{\partial x^2} - \bar{u}_B \frac{\partial \langle C\rangle^P}{\partial x} - \hat{m}_{met} = \left(f_{u(B)}(1-\varepsilon)K^* + \varepsilon\right)\frac{\partial \langle C\rangle^P}{\partial t} \tag{2.8}$$

where $\hat{m}_{met}$ is the hepatocellular metabolism rate normalized by the liver tissue volume (mgml^{-1} s^{-1}) given by Eqs. (2.3) and (2.4) for a constant and nonlinear hepatocellular metabolism, respectively. Accordingly, the intrinsic clearance function can be defined as:

$$Cl_{int} = \begin{cases} Cl_{int-invivo} & \text{if } Cl_{int} \neq f(C) \\ \dfrac{V_{\max}}{K_M + f_{u(B)}\langle C\rangle^P} & \text{if } Cl_{int} = f(C) \end{cases} \tag{2.9}$$

As indicated in Eq. (2.8), the time dependent drug concentration in both hepatocytes and plasma is described by the accumulation term on the right side of the equation. The liver structural characteristics of porosity and tortuosity are included in the governing equation while the blood Darcy velocity and the axial dispersion coefficient takes into account the influence of the tissue permeability. The initial plasma drug concentration of the liver tissue is zero and is defined as:

$$\langle C \rangle^P (x, t = 0) = 0 \tag{2.10}$$

If instantaneous drug distribution in the body occurs following intravenous (IV) bolus injection of drug then the ratio of the IV dose (X_0) to the volume of distribution (V_d) determines the plasma drug concentration at the blood entry to the liver. At the liver inlet and outlet boundaries the convective mass flow predominates and diffusion and dispersion are assumed to be insignificant. Consequently, the boundary conditions can be described as:

$$\begin{cases} \langle C \rangle^P (x = 0, t) = \dfrac{X_0}{V_d} \;\&\; D_{\parallel}^d (x = 0, t) = 0 \\ \left. \dfrac{\partial \langle C \rangle^P}{\partial x} \right|_{x = L, t} = 0 \quad \&\; D_{\parallel}^d (x = L, t) = 0 \end{cases} \tag{2.11}$$

When the drug distribution within the liver is complete, the model can predict the plasma unbound drug concentration just at the liver outlet in the hepatic vein. Knowledge of the drug concentration at the inlet and outlet of the liver allows the calculation of the hepatic clearance ($Cl_{h\text{-}LVA}$) as:

$$Cl_{h-LVA} = \frac{Q_h \left(\langle C_u \rangle^P \big|_{x=0} - \langle C_u \rangle^P \big|_{x=L} \right)}{\langle C_u \rangle^P \big|_{x=0}} \tag{2.12}$$

where $\langle C_u \rangle^P$ is the local volume averaged unbound drug concentration (mgml^{-1}), L is the equivalent length of the liver (m). In order to compare the proposed model to other models, the hepatic clearance was calculated for WS, PT and DP models, respectively, as follows (Ito and Houston, 2004):

$$Cl_{h-WS} = \frac{Q_h \; f_{u(B)} \, Cl_{int-invivo} V_t}{Q_h + V_t \, f_{u(B)} \, Cl_{int}} \tag{2.13}$$

$$Cl_{h-PT} = Q_h \left(1 - \exp\left(- \frac{f_{u(B)}\, Cl_{int-invivo}}{\frac{Q_h}{V_t}} \right) \right) \tag{2.14}$$

$$Cl_{h-DP} = Q_h \left(1 - \frac{4a}{(1+a)^2 \exp\left(\frac{(a-1)}{2D_n} \right) - (1-a)^2 \exp\left(\frac{-(a+1)}{2D_n} \right)} \right) \tag{2.15}$$

where $Cl_{h\text{-}WS}$, $Cl_{h\text{-}PT}$ and $Cl_{h\text{-}DP}$ (s^{-1}) are the hepatic clearance suggested by WS, PT and DP models, the dispersion number of D_n in Eq. (2.15) is 0.17 and a is defined as (Robert and Rowland, 1986):

$$a = \sqrt{1 + \frac{4 f_{u(B)} V_t Cl_{int-invivo} D_n}{Q_h}} \tag{2.16}$$

where V_t is the volume of the liver tissue (ml) and can be calculated for males and females by Eqs. (2.17) and (2.18), respectively, as a function of body weight as (Anderson et al., 2000):

$$V_t = 415 + 17.3 W_b + 210.5 \log(10 a_c) \tag{2.17}$$

$$V_t = 389 + 14.5 W_b \tag{2.18}$$

where V_t is the liver volume (ml), W_b is the body weight (kg) and a_c is the number of drinks per day. Because of a poorer correlation between liver volume and body weight suggested by the allometric model (Swift et al., 1978), Eqs. (2.17) or (2.18) were used for calculation of liver volume in this study. For nonalcoholic males and females, the average values of the liver volume are 1602 and 1341 ml, respectively (Anderson et al., 2000). With estimates of hepatic clearance (Cl_h) and the hepatic perfusion rate (Q_h), the bioavailability is calculated as (Roberts and Rowland, 1986):

$$F_H = 1 - \frac{Cl_h}{Q_h} \tag{2.19}$$

2.2.3 Numerical Solution of the model

Numerical solution of the model required a number of simplifying assumptions as follows:

i) Extrahepatic clearance of the drug was negligible;

ii) Biliary excretion of parent drug was negligible;

iii) Following IV administration drug undergoes instantaneous distribution in the body such that plasma drug concentration at the liver inlet could be assumed as the ratio of IV dose to the volume of distribution of the drug;

iv) Blood concentration to plasma concentration ratio of the drug was unity;

v) The unbound fraction of the drug in the blood remained unchanged with time;

vi) Radial dispersion was negligible compared to advection and axial dispersion.

The liver representative slab was divided into *N+1* nodes where *N* was the node at the liver outlet and *N+1* was a fictitious node just in the hepatic vein. Then, the governing equation, Eq. (2.8), was discretized using implicit finite difference method. Rearranging the finite difference equations resulted in the following system of algebraic equations as:

$$C_i^j = \frac{\alpha C_i^{j-1} + \beta C_{i+1}^j + (2+\gamma) C_{x=0}^j}{(3+\alpha+\gamma+\theta)} \qquad (\mathrm{i} = 1) \tag{2.20}$$

$$C_i^j = \frac{\alpha C_i^{j-1} + \left(\frac{3\beta}{16}\right)\left(C_{i+1}^j + C_{i-1}^j\right) + \left(\frac{\gamma}{2}\right) C_{i-1}^j}{\left(\alpha + \frac{3\beta}{8} + \frac{\gamma}{2} + \theta\right)} \qquad (1 \le \mathrm{i} \le N) \tag{2.21}$$

$$C_i^j = \frac{\alpha C_i^{j-1} - \left(\frac{3\beta}{8}\right) C_{i-1}^j + \left(\frac{\gamma}{2}\right) C_{i-1}^j}{\left(\alpha - \frac{3\beta}{8} + \frac{\gamma}{2} + \theta\right)} \qquad (\mathrm{i} = N+1) \tag{2.22}$$

where *i* is the node index, *j* is the time step index, *C* represents the plasma unbound drug concentration, and the coefficients of α, β, γ, and θ are defined as:

$$\alpha = \frac{(1-\varepsilon)K^* + \left(\frac{\varepsilon}{f_{u(B)}}\right)}{\Delta t}$$

$$\beta = \frac{16\left(\frac{D_{\parallel}^{d}}{f_{u(B)}} + \frac{D_{AB}\varepsilon}{\tau}\right)}{3\Delta x^2}$$

$$\theta = \begin{cases} Cl_{int-invivo} & \text{if } Cl_{\text{int}} \neq f(C) \\ \frac{V_{\max}}{K_M + C_i^{j-1}} & \text{if } Cl_{\text{int}} = f(C) \end{cases} \qquad (2.23)$$

$$\gamma = \frac{2\bar{u}_B}{f_{u(B)}\Delta x}$$

The mesh size was determined based on the sensitivity analysis of the drug concentration gradient across the liver at the time when drug distribution in the liver reaches a distribution equilibrium (i.e. at 100 s) with respect to the number of nodes. Time step size was determined based on the sensitivity of the stability, accuracy and the speed of solution with respect to the time step size at different mesh size. Gauss-Seidel iterative method with a convergence criterion of 10^{-6} was used for solving the system of algebraic equations simultaneously.

2.2.4 Pharmacokinetic and structural parameters for the simulation

Simulation was performed for eight drugs, naloxone, lidocaine, metoprolol, verapamil, caffeine, timolol, diazepam, and phenacetin (Shibata et al., 2002), at a hepatic perfusion rate of 1500 mlmin^{-1} and a sinusoidal porosity of 0.12 (Smye et al., 2007) for a time-course of 200 s following a 5 mg IV dose of each drug. The tortuosity of the liver tissue was calculated according to the tortousity of porous media consisting of layer by layer parallel rods as (Perry and Green, 1997):

$$\tau = \frac{(1-\varepsilon)^2}{\varepsilon} \tag{2.24}$$

Table 2.1 shows the pharmacokinetic properties of each drug used for the simulation. The unbound fraction and intrinsic clearance of the drugs vary from 0.013 (diazepam) to 0.883 (metoprolol), and from 0.3 (diazepam) to 154.9 (nalaxone) $mlmin^{-1}kg^{-1}$, respectively. Lidocaine, with a tissue partition coefficient of 0.61 (Joseph et al., 2001), was chosen as a candidate for the simulation of drug distribution across the liver as well as for sensitivity analyses.

Table 2.1. Pharmacokinetic parameters of drugs used in the simulation of hepatic clearance.

Drug	*Unbound fraction*	*Intrinsic clearance ($mlmin^{-1}kg^{-1}$)*	*Volume of distribution (Lkg^{-1})*
Lidocaine	0.615 [a]	29.8 [g]	3.00 [h]
Nalaxone	0.559 [b]	154.9 [b]	2.64 [i]
Metoprolol	0.883 [c]	17.8 [c]	4.5 [j]
Verapamil	0.280 [d]	31.0 [d]	4.63 [k]
Caffeine	0.650 [e]	1.7 [e]	1.06 [l]
Phenacetin	0.600 [f]	127.5 [f]	1.55 [m]
Timolol	0.400 [o]	7.7 [o]	3.5 [n]
Diazepam	0.013 [p]	0.3 [p]	1.57 [q]

[a] Jacobi et al., 1983; [b] Asali and Brown, 1984; Holford, 1998; [c] Regardh et al., 1981; [d] Deshmukh and Harsch, 2011; [e] Blanchard, 1982; [f, m] Raaflaub and Dubach, 1975; [g] Wing et al., 1984; Remmel et al., 1991; [h] Ikeda et al., 2010; [i] Glass et al., 1994;; [j] Hardman et al., 1996; [k] McAllister and Kirsten, 1982; [l] Lelo et al., 1986; [n] Else et al., 1978; [o] Holford, 1998; [p] Divoll et al., 1983; [q] Norman et al., 1997

2.3. Results and discussion

In order to determine the optimum mesh size, the sensitivity of the drug concentration gradient across the liver to the grid size at 100 s was investigated. Figure 2.3 depicts the plasma drug concentration with the liver equivalent length for different mesh grid numbers. According to Figure 2.3, the drug concentration gradient across the liver increases sharply with the number of nodes up to 200. Thereafter, the concentration gradient increases marginally up to 350 nodes and then remains relatively unchanged. A mesh size of 0.63 mm equivalent to 350 nodes was

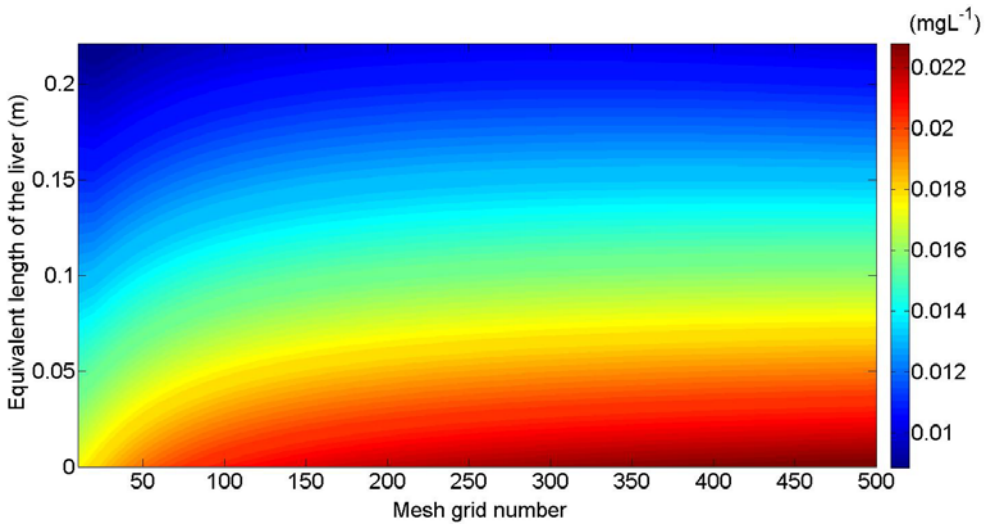

Figure 2.3. Sensitivity analysis for determination of optimum mesh size for the numerical solution.

adopted for the numerical solution. According to accuracy and speed of solution, which were performed for different time step sizes of 0.1, 1, 5, and 10 s, a time step size of 1 s was adopted for the numerical solution.

Figure 2.4 illustrates the correlation between the predicted values of hepatic clearance and observed values reported by Shibata et al. (2002) for eight drugs at a perfusion rate of 1500 $mlmin^{-1}$ for a 70 kg male subject. The coefficient of determination (R^2) of 0.91 indicates a good agreement between predicted and experimental values. The proposed model seems to underestimate the hepatic clearance of timolol and verapamil while overestimating phenacetin (Figure 2.4). This may be due to variability in the measured values of unbound drug fraction and intrinsic clearance, which will enhance uncertainty in the predicted values of hepatic clearance. For instance, the genetic polymorphism associated with timolol hepatocellular metabolism segregates a portion of the population into a poor metabolizer phenotype and estimates of timolol hepatic clearance causing a significant variability in the population. Since the pharmacokinetic properties used for the simulation are not population based, the predicted values may not capture

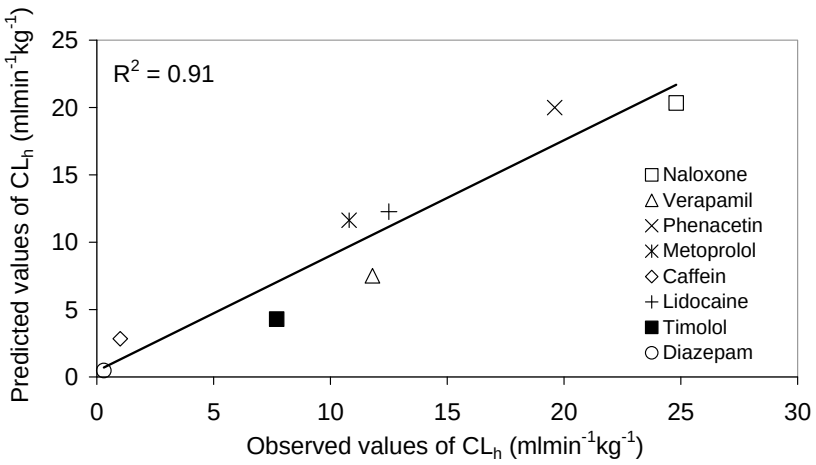

Figure 2.4. Predicted values of hepatic clearance from Porous Media based model versus reported observations (Shibata et al., 2002) for eight drugs.

the population variability and, hence, are associated with greater uncertainty in the estimation of the hepatic clearance of timolol.

Table 2.2 presents the observed values of the hepatic clearance of eight drugs as well as the predicted values from the proposed porous media (PM) based model and the WS, PT and DP models. Table 2.2 indicates that PM model predictions are mostly consistent with PT and DP models and relatively less consistent with the WS model, likely due to the oversimplifications associated with WS model. A comparison of observed values to the predicted values of the models indicates that the PM model is less predictive of caffeine hepatic clearance while more predictive for diazepam hepatic clearance relative to the WS, PT and DP models.

Figure 2.5 illustrates the correlation between the predicted and the reported values of bioavailability for eight drugs at a hepatic perfusion rate of 1500 $mlmin^{-1}$ for a 70 kg male subject. The coefficient of determination (R^2) of 0.80 indicates a relatively good agreement between predicted and observed values of bioavailability, although PM model overestimates verapamil and timolol and underestimates naloxone, metoprolol, and phenacetin. Since the bioavailability is calculated based on the hepatic clearance, Eq. (2.19), the error associated with

Table 2.2. Comparison of model predictions with observed values of the hepatic clearance associated with seven drugs.

	Model predictions of Cl_H (ml/min.kg)				*Observations*
Compound	*PM*	*WS*	*PT*	*DP*	*reported* [a]
Naloxone	20.34	17.18	21.05	20.20	24.8
Verapamil	7.51	6.18	7.14	6.84	11.8±5.0
Phenacetin	20.00	16.74	20.83	19.83	19.6±4.5
Lidocaine	12.27	9.88	12.32	11.51	12.5±1.5
Metoprolol	11.63	10.14	12.70	11.86	10.8±1.5
Caffeine	2.83	1.05	1.08	1.07	1.0±0.4
Timolol	4.29	3.11	3.28	3.35	7.7±1.2
Diazepam	0.47	0.01	0.01	0.01	0.3±0.1

[a] Shibata et al., 2002

the predicted hepatic clearance accumulates in the predicted values of bioavailability. For instance, predicted hepatic clearance accumulates in the predicted values of bioavailability. For instance, underestimation of hepatic clearance of verapamil and timolol leads to the overestimation of their bioavailability. Furthermore, the literature reports bioavailability following oral administration with reductions in bioavailability resulting from intestinal and hepatic mechanisms. The PM model only accounts for drug loss by the liver in its prediction of bioavailability.

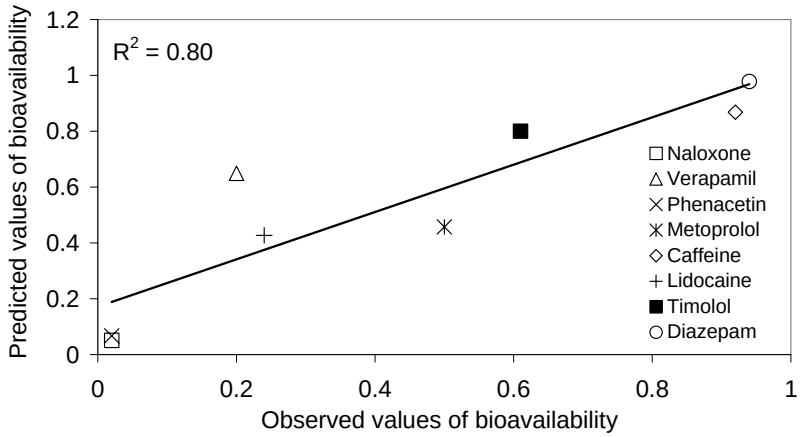

Figure 2.5. Predicted values of bioavailability from Porous Media based model versus reported observations (Shibata et al., 2002) for eight drugs.

Table 2.2 presents the observed values of bioavailability of eight drugs as well as the predicted values from the proposed porous media (PM) based model and the WS, PT and DP models. Table 2.3 indicates that bioavailability predictions from the PM model show good agreement with the DP model while a significant discrepancy can be distinguished between PM and WS models. The comparison of predicted values with the reported data of bioavailability shows that the WS model substantially overestimates drug bioavailability.

Table 2.3. Comparison of model predictions with observed values of bioavailability associated with seven drugs.

	Model predictions of Bioavailability (F_H)				*Reported*
Compound	*PM*	*WS*	*PT*	*DM*	*observations*[a]
Naloxone	0.051	0.198	0.018	0.057	0.02
Verapamil	0.649	0.712	0.667	0.681	0.2±0.12
Phenacetin	0.067	0.219	0.028	0.074	0.02±0.03
Lidocaine	0.427	0.539	0.425	0.463	0.24±0.05
Metoprolol	0.457	0.577	0.480	0.512	0.5±0.11
Caffeine	0.868	0.951	0.950	0.950	0.92±0.04
Timolol	0.800	0.855	0.844	0.847	0.61±0.06
Diazepam	0.978	0.990	0.990	0.990	0.94±0.2

[a] Shibata et al., 2002

Table 2.4 shows mean squared prediction errors (MSE) associated with PM, WS, PT and DP models for hepatic clearance and bioavailability. It indicates that PM model results in smaller MSE for hepatic clearance predictions compared to the other models and the WS, which is a physiologically oversimplified model, leads to significantly larger MSE associated with hepatic clearance predictions. PM, PT and DP models result in similar MSE while WS causes larger MSE for bioavailability predictions. Unlike MSE values, all models have close coefficient of determination values for hepatic clearance and bioavailability. Since the proposed numerical model takes into account more structural (i.e. porosity, tortousity) and physico-chemical parameters (i.e. tissue partition coefficient) compared to the other models, errors associated with the parameters are expected to propagate in the solution resulting in larger uncertainties in

predictions. However, lower MSE of hepatic clearance predictions and the same MSE of bioavailability predictions along with similar coefficient of determination values as other models suggest an improvement in mechanistic modeling of hepatic drug elimination using the LVA method.

Table 2.4. Mean squared prediction error (MSE) and coefficient of determination (R2) values of hepatic clearance and bioavailability for well-stirred, parallel tube, dispersion and porous media models.

	MSE		R^2	
Model	*Hepatic clearance*	*Bioavailability*	*Hepatic clearance*	*Bioavailability*
Porous media	7.74	0.04	0.91	0.80
Well stirred	18.41	0.06	0.92	0.82
Parallel tube	8.15	0.04	0.91	0.81
Dispersion	9.42	0.04	0.92	0.81

Figure 2.6 depicts the effect of the axial dispersion on the plasma unbound drug concentration gradient across the liver at different times. In the absence of axial dispersion, diffusion and convection mass transfer are the only mechanisms of drug transport in the liver. As observed from Fig. 2.6a, drug is distributed in the liver by the molecular diffusion and the advection associated with the blood flow so that the drug can only be distributed within 12 cm of the liver in 10 s while hepatocellular drug metabolism is taking place in the liver. After 20 s the drug reaches the hepatic vein at the liver outlet and drug concentration begins rising until it reaches steady state at 80 s. Unlike advection and diffusion, axial dispersion causes the drug to stretch along the liver within seconds. As seen in Fig. 2.6b, the drug reaches the hepatic vein at the liver outlet in less than 10 s. In other words, axial dispersion causes the drug to experience less residence time during which hepatocellular metabolism of the drug takes place in the liver. Less residence time can cause an inadequate time for the drug to reach equilibrium with hepatocytes, which, in turn, can reduce the first pass effect within the initial distribution time.

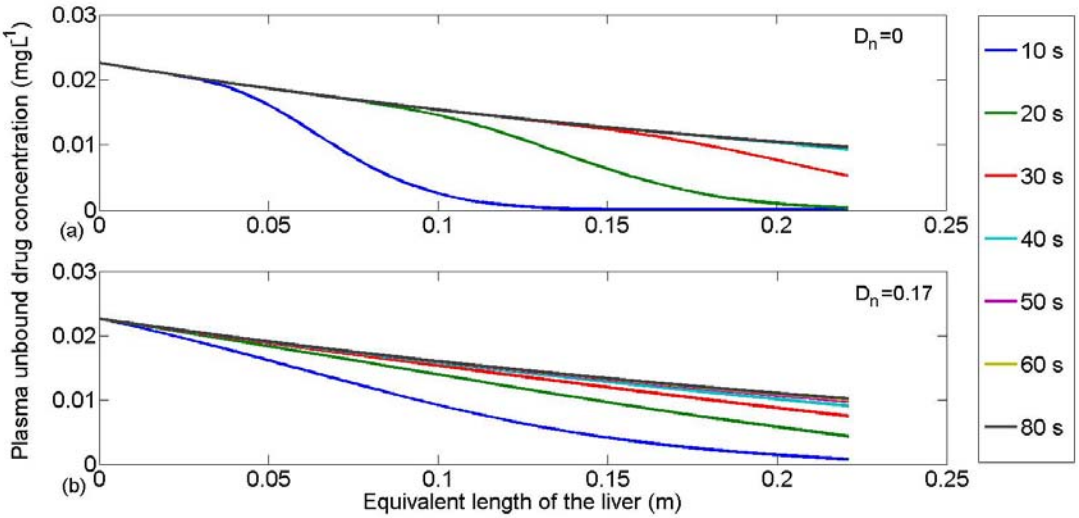

Figure 2.6. Plasma unbound drug concentration gradient across the liver at different times in the absence (a) and presence (b) of axial dispersion (Dn) for lidocaine.

Figure 2.7 illustrates the variation of plasma drug concentration at the liver outlet in the hepatic vein with time and axial dispersion number. For low levels of axial dispersion, the residence time of the drug is about 17 s when the drug reaches the liver outlet followed by a sharp increase in the plasma drug concentration. However, as the dispersion number increases the residence time of drug in the liver decreases such that at higher dispersion numbers it takes only a few seconds for the drug to leave the liver while the plasma drug concentration gradually increases at the hepatic vein. The simulated residence time has good agreement with the dispersion model predictions of residence time of a drug bolus in the liver reported by Roberts and Rowland (1986).

Figure 2.8 illustrates the sensitivity of the drug concentration gradient across the liver to the porosity of the liver at an axial dispersion number of 0.17. An increase in the liver porosity causes the plasma drug concentration to elevate across the liver. Likewise, decreases in liver porosity results in reductions in the plasma drug concentration across the liver due to the effect of the porosity on the sinusoidal blood velocity (pore velocity), which is obtained by the ratio of

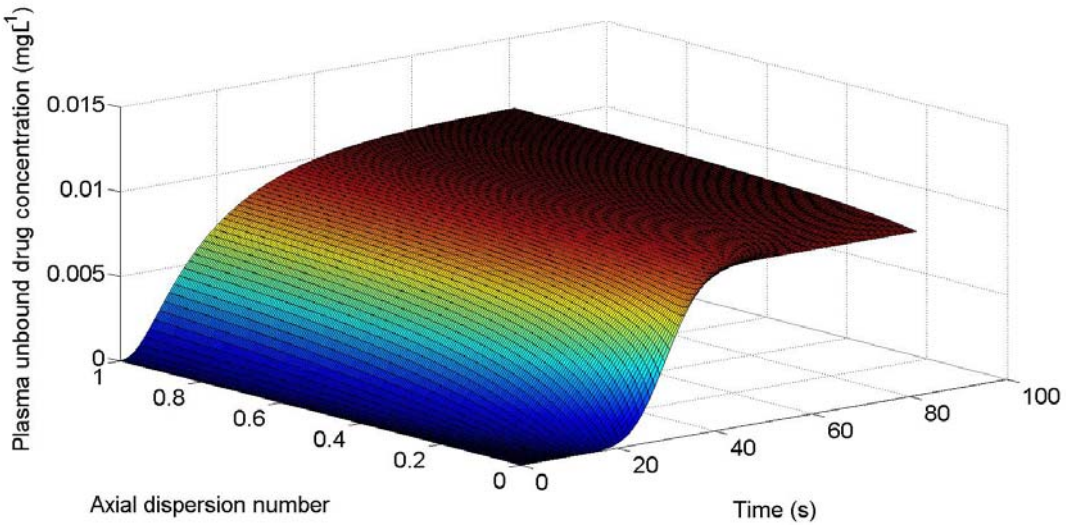

Figure 2.7. Variation of plasma unbound drug concentration at the hepatic vein versus time and axial dispersion number for lidocaine.

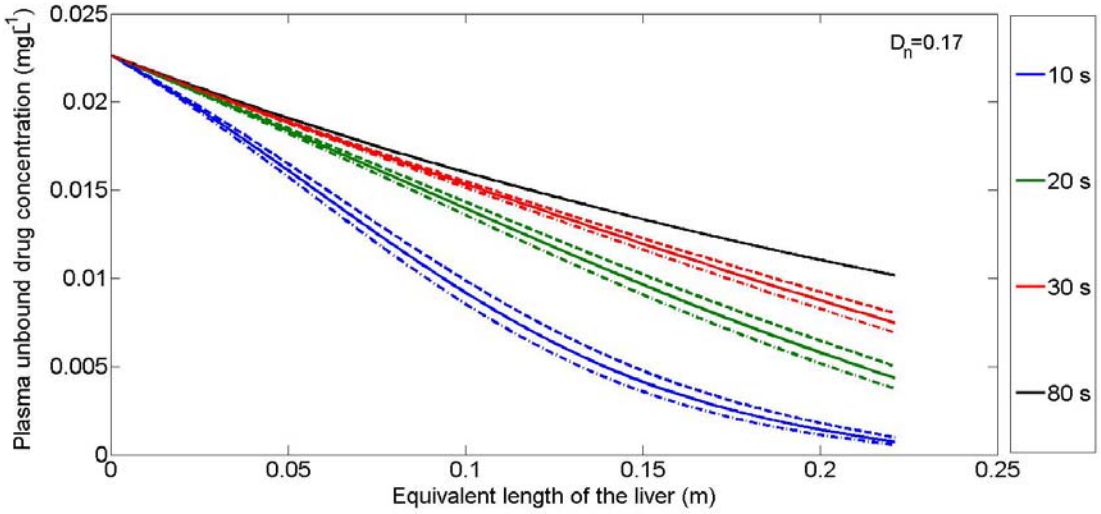

Figure 2.8. The influence of porosity on plasma unbound drug concentration gradient across the liver at different times for lidocaine for axial dispersion number (D_n) of 0.17: – –, ε=0.06; ——, ε=0.12; – · –, ε=0.18.

blood Darcy velocity to the porosity. Lower sinusoidal porosity leads to higher pore velocity enhancing the effect of the advection term in Eq. (2.8). Larger advection causes the drug to move forward faster so that the residence time is reduced and the drug concentration at any position across the liver increases during the transient distribution time. Likewise, higher porosity reduces the plasma drug concentration at any position during the unsteady state period across the liver; however, the effect of porosity on the concentration gradient becomes insignificant at 80 s (Fig. 2.8).

Figure 2.9 depicts the sensitivity of the plasma drug concentration gradient across the liver to the tissue partition coefficient of lidocaine. Lidocaine's large tissue partition coefficient results in smaller plasma drug concentrations across the liver at all distribution times of the drug. According to the definition of the tissue partition coefficient (the ratio of the drug concentration in hepatocytes to that in plasma), the larger tissue partition coefficient implies that a larger fraction of unbound drug is partitioned into hepatocytes where the drug is metabolized. Therefore, for larger hepatic partition coefficient, plasma unbound drug concentration is expected to decrease across the liver during the transient drug distribution (Fig. 2.9). However, once drug distribution in the liver reaches steady state at 80 s, the effect of tissue partition coefficient becomes insignificant. Mathematically this occurs because the accumulation term in the right side of the governing equation (Eq. (2.8)) becomes zero at steady state where the effect of the tissue partition coefficient is canceled in the model. In other words, the magnitude of the tissue partition coefficient has an influence on how fast drug distribution across the liver reaches equilibrium.

Figure 2.10 depicts the affect of intrinsic clearance (Fig. 2.10a) and drug unbound fraction (Fig. 2.10b) on the plasma drug concentration gradient across the liver for lidocaine at the axial

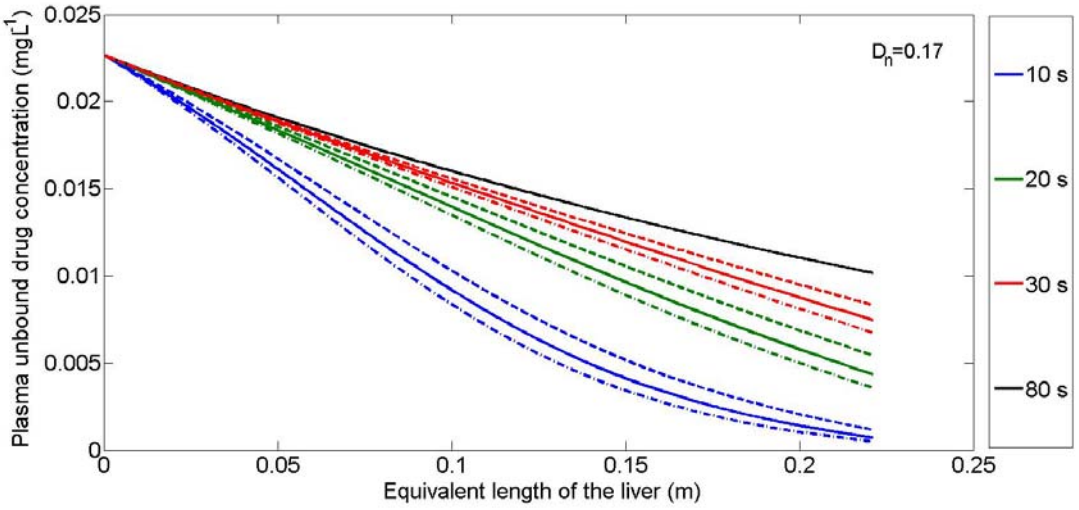

Figure 2.9. Sensitivity of plasma unbound drug concentration gradient across the liver to the partition coefficient for lidocaine for axial dispersion number (D_n) of 0.17: – · –, K^*=0.70; ——, K^*=0.61; – –, K^*=0.40.

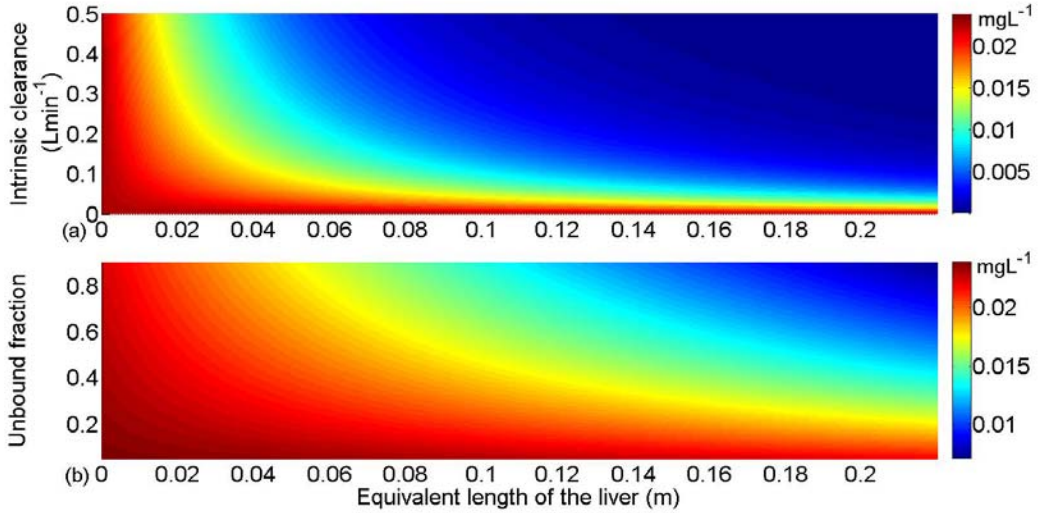

Figure 2.10. Influence of intrinsic clearance (a) and unbound fraction (b) on plasma unbound drug concentration gradient across the liver for lidocaine at an axial dispersion number of 0.17.

dispersion number of 0.17. At an unbound fraction of 0.615, the concentration gradient of lidocaine across the liver is insignificant for low intrinsic clearance values from 0 to 0.05 $Lmin^{-1}$. This implies that hepatocellular metabolism of the drug is so low that its concentration remains relatively unchanged across the liver. However, as intrinsic clearance is enhanced from 0.05 to

0.15 $Lmin^{-1}$, the plasma drug concentration gradient dramatically increases. If the intrinsic clearance is increased further, the plasma drug concentration in the second half of the liver is significantly reduced so that for intrinsic clearance values greater than 0.2 $Lmin^{-1}$ the drug concentration at the liver outlet is zero implying that all drug is eliminated across the liver. Unlike the second half of the liver, the first half of the liver demonstrates more sensitivity to higher values (>0.2 $Lmin^{-1}$) of the intrinsic clearance. Mathematically this is explained by Eq. (2.3) where hepatocellular metabolism is a function of both intrinsic clearance and unbound drug concentration such that high intrinsic clearance values result in very low unbound drug concentrations in the second half of the liver. Hence, in the second half of the liver, despite high intrinsic clearance values the rate of metabolism is very low due to very small plasma drug concentrations and remains insensitive to intrinsic clearance. However, the first half of the liver is subjected to drug enriched blood of the portal vein and hepatic artery and the plasma drug concentration is sufficiently high to be sensitive to the higher values of intrinsic clearance.

Figure 2.10b illustrates the sensitivity of the plasma unbound drug concentration across the liver to the unbound fraction of lidocaine at an intrinsic clearance of 29.8 $mlmin^{-1}kg^{-1}$. With higher values of unbound drug fraction, the plasma drug concentration gradient increases so that for unbound fractions greater than 0.8 the plasma drug concentration at the last 2 cm of the liver is very small. Comparing Fig. 2.10a to Fig. 2.10b indicates that the drug concentration gradient across the liver dramatically increases with increases in intrinsic clearance while the unbound fraction has a relatively negligible effect on the drug concentration gradient along the liver compared to the intrinsic clearance. In addition, no significant change in drug concentration occurs in the first 1 cm of liver length when the intrinsic clearance and unbound fraction are increased. The dispersion of the drug enriched blood at the region close to the liver inlet

suppresses the impact of higher intrinsic clearance and unbound fraction values on the concentration gradient in this portion of the liver.

Figure 2.11 illustrates the variation of hepatic clearance with respect to the hepatic perfusion rate and intrinsic clearance. At low values of intrinsic clearance from 0.01 to 0.1 $Lmin^{-1}$ kg^{-1} hepatic perfusion rate has no significant effect on hepatic clearance when perfusion rate increases from 1100 to 1800 $mlmin^{-1}$; however, small changes in intrinsic clearance induce sharp increases in hepatic clearance. This suggests that for low intrinsic clearance values the limiting factor of hepatic clearance is the hepatocellular enzyme activity represented by the intrinsic clearance. For values of the intrinsic clearance greater than 0.1 $Lmin^{-1}kg^{-1}$ the effect of enzyme activity on hepatic clearance becomes insignificant while hepatic clearance increases with

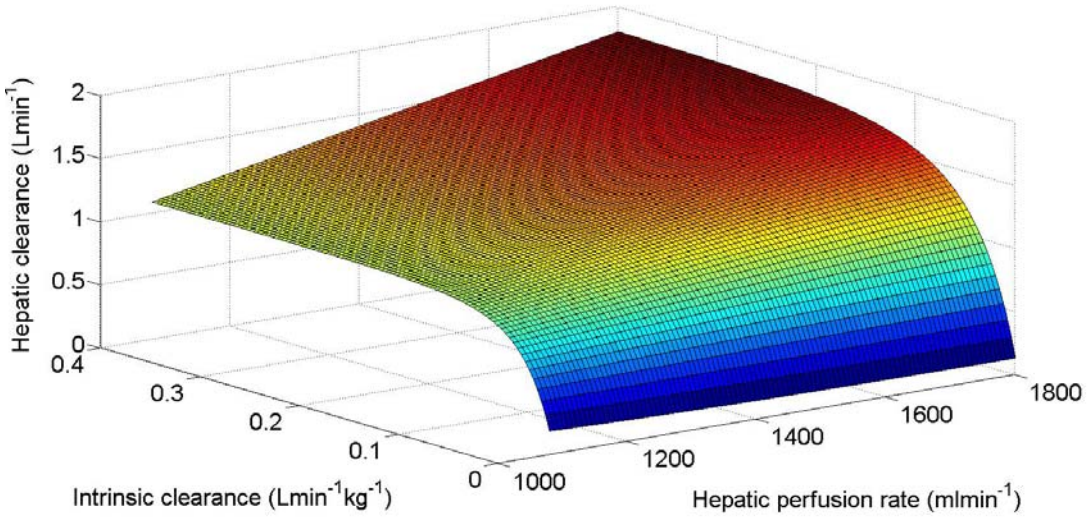

Figure 2.11. Variation of hepatic clearance with intrinsic clearance and hepatic perfusion rate for lidocaine at a sinusoidal porosity of 0.12 and perfusion rate of 1500 $mlmin^{-1}$.

hepatic perfusion rate. This suggests that at higher values of intrinsic clearance the speed of drug presentation to the hepatocytes that is determined by perfusion rate is the limiting factor for hepatic clearance.

Figure 2.12 depicts the influence of the hepatic perfusion rate and intrinsic clearance on the hepatic bioavailability of lidocaine. At very low intrinsic clearance values (less than 0.05 $Lmin^{-1}kg^{-1}$) hepatic bioavailability is high for all hepatic perfusion rates; the effect of the intrinsic clearance predominates although, increasing perfusion rates result in slight increases in bioavailability at low intrinsic clearance values. This is likely due to shorter residence times of the drug in the liver at higher perfusion rates, which reduces the equilibration time between the plasma and hepatocytes. As intrinsic clearance values increase bioavailability decreases dramatically such that for intrinsic clearance values greater than 0.2 $Lmin^{-1}kg^{-1}$ bioavailability approaches zero implying all drug is metabolized by the liver during its first pass across the liver.

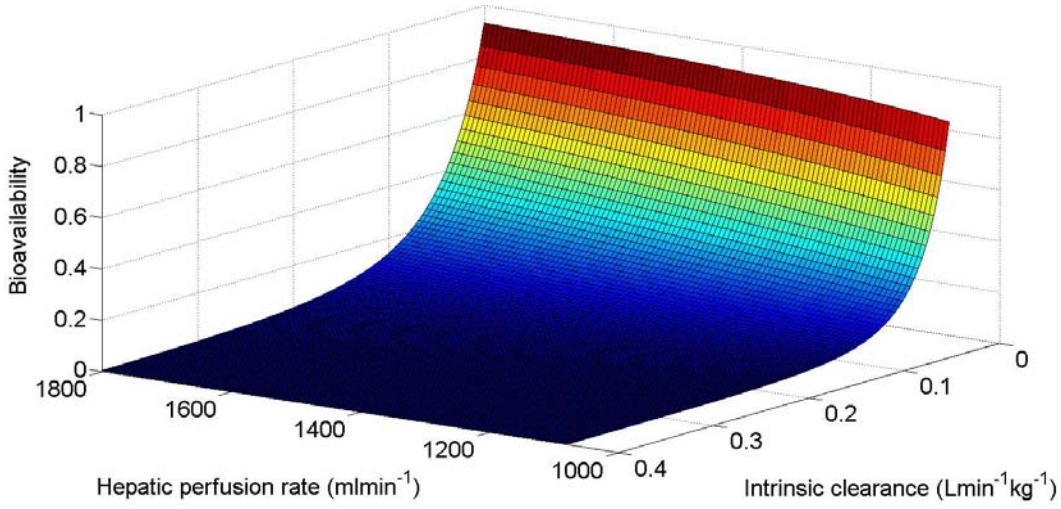

Figure 2.12. Variation of bioavailability with intrinsic clearance and hepatic perfusion rate for lidocaine at a sinusoidal porosity of 0.12 and perfusion rate of 1500 $mlmin^{-1}$.

Figure 2.13 illustrates the sensitivity of bioavailability to the intrinsic clearance and the unbound drug fraction. For very low values of unbound fraction (<0.1) or intrinsic clearance (<0.1 $Lmin^{-1}kg^{-1}$) bioavailability gradually decreases with any increases in either unbound fraction or intrinsic clearance. According to Eq. (2.3) which relates the metabolism rate to the

intrinsic clearance and unbound fraction, when unbound fraction and intrinsic clearance are very low, an increase in only one does not produce a substantial drop in bioavailability due to the suppressing effect of the low value of the other variable. However, for higher values (>0.15) of unbound fraction and intrinsic clearance, an increase in either one causes a significant drop in bioavailability implying that metabolism rate is sufficiently sensitive to the magnitude of the values of either unbound fraction or intrinsic clearance. Bioavailability approaches zero when unbound fraction and intrinsic clearance gain values greater than 0.5 and 0.2 $Lmin^{-1}kg^{-1}$, respectively.

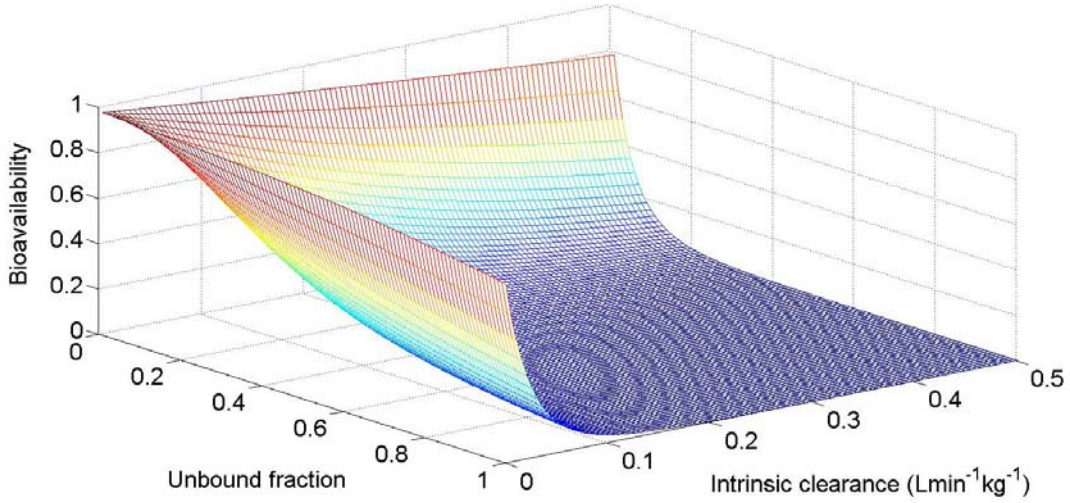

Figure 2.13. Variation of bioavailability with intrinsic clearance and unbound fraction for lidocaine at a sinusoidal porosity of 0.12 and perfusion rate of 1500 $mlmin^{-1}$.

The proposed PM model was executed to predict the variation of concentration dependent intrinsic clearance across the liver for 1'-hydroxymidazolam (1OH-MDZ) with an affinity term (K_m) of 0.752 mgL^{-1}, maximum hepatocellular metabolism rate (V_{max}) of 0.00173 mg $L^{-1}s^{-1}$ and tissue partition coefficient of 1.25 (Willmann and Edginton, 2007). Figure 2.14 depicts the variation of intrinsic clearance and plasma unbound drug concentration with position and time across the liver. In Fig. 2.14a, an exponentially increasing trend of the intrinsic clearance can be

observed across the liver for all time points during transient drug distribution in the liver. The variation of intrinsic clearance is consistent with the plasma unbound drug concentration gradient (Fig. 2.14b) and the intrinsic clearance function, Eq. (2.9). In Fig. 2.14b, drug concentration is high in the first 8 cm of the liver due to its short distance from the liver inlet where the liver receives a drug enriched blood supply; however, the concentration decreases sharply along the rest of the liver. According to Eq. (2.9), for concentration dependent intrinsic clearance, a lower drug concentration results in a smaller denominator forcing the proportionality to increase dramatically as observed in Fig. 2.14a. Subsequently, concentration-dependent intrinsic clearance can be observed at all times during drug distribution. The drug concentration across the liver increases with time (Fig. 2.14b) causing intrinsic clearance to decrease accordingly (Fig. 2.14a). As drug distribution across the liver approaches steady state conditions after 40 s, the change in the intrinsic clearance becomes insignificant; however, a nonlinear variation of intrinsic clearance across the liver occurs all the time. Unlike the proposed PM model, WS, PT

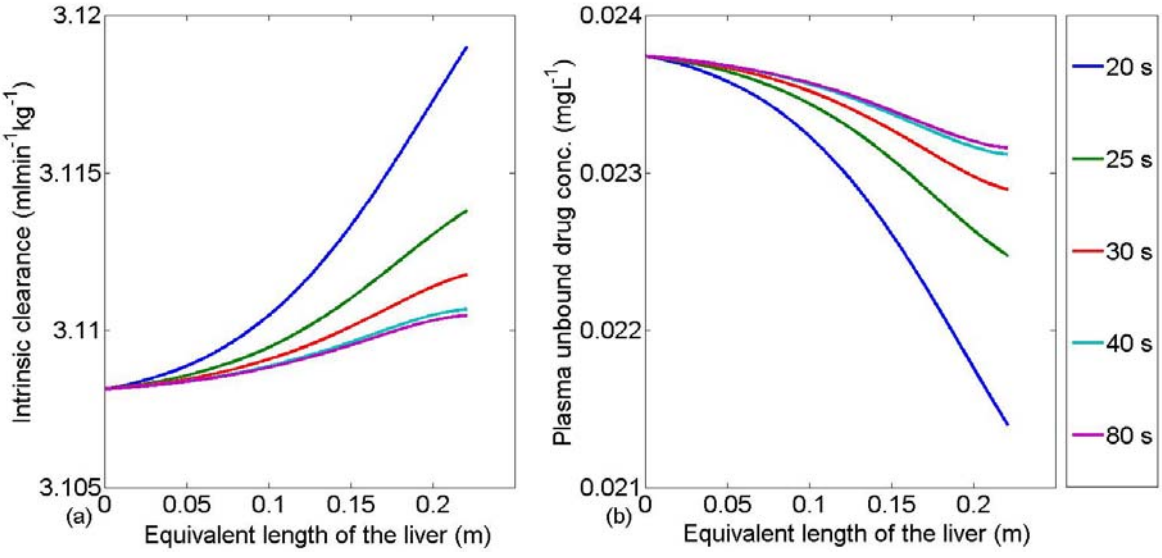

Figure 2.14. Variation of intrinsic clearance (a) and plasma unbound drug concentration of 1-hydroxymidazolam across the liver at different times.

and DP models are unable to predict concentration dependent intrinsic clearance so that an uncertainty will exist in the predictions. In addition, as the affinity term value of 0.752 mgL^{-1} is comparable to the lowest drug concentration (0.02103 mgL^{-1}) occurring at 20 s in the liver outlet, the influence of the drug concentration on the magnitude of the denominator of Eq. (2.9) cannot be neglected. Therefore, the simulation of the hepatic drug elimination of 1OH-MDZ must take into account the concentration dependent intrinsic clearance.

2.4. Conclusion

According to the liver permeability, sinusoidal diameter, the size of acinus and the liver equivalent length, the validity condition of LVA method was satisfied by the length scales of the liver tissue as a porous medium. Applying LVA method and local equilibrium, a governing equation taking into account the liver structural characteristics, the drug physico-chemical properties and the mass transport properties was developed and validated using reported observations of hepatic clearance (R^2=0.91) and oral bioavailability (R^2=0.80) of eight drugs. The proposed model suggests similar coefficient of determination values but smaller MSE for predicted values of hepatic clearance compared to WS, PT and DP models. MSE values of bioavailability are similar between PT, DP and the proposed mechanistic model; however, WS model possesses a larger MSE.

The simulation of drug distribution at different levels of axial dispersion numbers indicates that the influence of axial dispersion on the drug concentration gradient and residence time of the drug across the liver is very significant. Therefore, excluding the axial dispersion from a model (i.e. WS and PT) can inherently cause an uncertainty in model predictions. A sensitivity analysis revealed that an increase in the liver porosity, which reduces the sinusoidal pore velocity of the

blood, causes the drug concentration gradient to decrease across the liver. The analysis also shows that an increase in the hepatic tissue partition coefficient elevates the drug concentration gradient across the liver and the drug concentration gradient across the liver is very sensitive to intrinsic clearance such that hepatic drug elimination in the second half of the liver dramatically increases with the intrinsic clearance. Although the influence of unbound fraction on the drug concentration gradient is appreciable, the effect of intrinsic clearance is significantly higher than the unbound fraction. The analysis also indicates that the influence of perfusion rate on the hepatic clearance becomes distinctive at larger values of intrinsic clearance while no limiting effect of the perfusion rate is observed at low intrinsic clearance.

Sensitivity analysis revealed that the bioavailability is sensitive to the interaction between unbound fraction and intrinsic clearance. For very low values of unbound fraction and intrinsic clearance, if either one is increased, the low value of the other variable suppresses the effect of the other one. However, with higher values a significant drop in bioavailability is observed with increases in either intrinsic clearance or unbound fraction. However, when the values are sufficiently high, bioavailability approaches zero and is insensitive to unbound fraction and intrinsic clearance.

Unlike WS, PT and DP models, the proposed PM model takes into account the nonlinear-concentration dependent intrinsic clearance based on which the effect of changes of drug concentration on the hepatocellular metabolism and hepatic drug elimination can be more precisely analyzed. In addition, the uncertainty associated with the assumption of a constant intrinsic clearance across the liver is minimized using PM model.

References

Anderson V., Sonne J., Sletting S. and Prip A. 2000. Volume of the liver in patients correlates to body weight and alcohol consumption *Alcohol & Alcoholism* 35 531-2.

Asali L. A. and Brown K. F. 1984. Naloxone protein binding in adult and foetal plasma *Eur. J. Clin. Pharmacol.* 27 459-63.

Bass L., Robinson P. J. and Bracken A. J. 1978 Hepatic elimination of flow substances: The distributed model *J. Theor. Biol.* 72 161-84.

Blanchard J. 1982. Protein binding of caffeine in young and elderly males. *J. Pharm. Sci.* 71:1415-1418.

Charles Y., Lee C. and Rubinsky B. 1989. A multi-dimensional model of momentum and mass transferrin the liver *Int. J. Heat Mass Transfer* 32 2421-34.

Deshmukh S. V. and Harsch A. 2011. Direct determination of the ratio of unbound fraction in plasma to unbound fraction in microsomal system (fup/fumic) for refined prediction of phase I mediated metabolic hepatic clearance *J. Pharmacol. Toxicol.* 63 35-9.

Divoll M., Greenblatt D. J., Ochs H. R. and Shader R. I. 1983. Absolute bioavailability of oral and intramuscular diazepam: effects of age and sex *Anesth Analg* 62 1-8.

Else O. F., Sorenson H. and Edwards I. R. 1978. Plasma timolol levels after oral and intravenous administration *Eur. J. Clin. Pharmacol.* 14 431-4.

Forker E. L. and Luxon B. 1978. Hepatic transport kinetics and plasma disappearance curves: Distributed modelling versus conventional approach *Am. J. Physiol.* 235 648-60.

Glass P. S., Jhaveri R. M. and Smith L. R. 1994. Comparison of Potency and Duration of Action of Nalmefene and Naloxone *Anesth. Analg.* 78 536-41.

Hardman J. G., Limbird L. E., Molinoff P. B., Ruddon R. W. and Gilman A. G. 1996. Goodman & Gilman's The Pharmacological Basis of Therapeutics McGraw-Hill, New York.

Holford N. 1998. Clinical Pharmacokinetics: Drug Data Handbook. 3rd ed ADIS Press Limited Auckland New Zealand.

Hisaka A. and Sugiyama Y. 1998. Analysis of nonlinear and nonsteady state hepatic extraction with the dispersion model using the finite difference method *J. Pharmacokinet. Biopharm.* 26 495-519.

Ito K. and Houston B. 2004. Comparison of the use of liver models for predicting drug clearance using in vitro kinetic data from hepatic microsomes and isolated hepatocytes *Pharm. Res.* 2 785-92.

Ikeda Y., Oda Y., Nakamura T., Takahashi R., Miyake W., Hase I. and Asada A. 2010. Pharmacokinetics of lidocaine, bupivacaine, and levobupivacaine in plasma and brain in awake rats *Anesthesiology* 112 1396-1403.

Jacobi J., NcGory R. W., McCoy H. and Matzke G. R. 1983. Hemodialysis clearance of total and unbound lidocaine *Clin. Pharm.* 2 54-7.

Jones A. L. and Spring-Mills E. 1988. The liver and gall bladder. In Cell and Tissue Biology, 6th ed (Edited by L. Weiss) Urban & Schwarzenberg Baltimore MA.

Joseph A. G., Jürgen V. and Joseph P. O. 2001. Prediction of lidocaine tissue concentrations following different dose regimes during cardiac arrest using a physiologically based pharmacokinetic model *Resuscitation* 50 331-40.

McAllister R. G. and Kirsten E. B. 1982. The pharmacology of verapamil: IV Kinetic and dynamic effects after single intravenous and oral doses *Clin. Pharmacol. Ther.* 31 418-26.

Lelo A., Birkett D. J., Robson R. A. and Miners J. O. 1986. Comparative pharmacokinetics of caffeine and its primary demethylated metabolites paraxanthine, theobromine and theophylline in man *Br. J. Clin. Pharmacol.* 22 177-82.

Norman W. M., Court M. H. and Greenblatt D. J. 1997. Age-related changes in the pharmacokinetic disposition of diazepam in foals *Am. J.Vet. Res.* 58 878-80.

Pang K. S. and Rowland M. 1977. Hepatic clearance of drugs. 1. Theoretical considerations of a well-stirred model and a parallel tube model: Influence of hepatic blood flow, plasma and blood cell binding and hepatocellular enzymatic activity on hepatic drug clearance *J. Pharmacokin. Biopharm.* 5 625-53.

Perry R. H. and Green D. W. 1997. Perry's chemical engineering handbook. 7th ed., McGraw-Hill, New York.

Raaflaub J. and Dubach U. C. 1975. On the pharmacokinetics of phenacetin in man *Eur. J. Clin. Pharmacol.* 8 261-65.

Regardh C. G., Jordo L., Ervik M., Lundborg P., Olsson R. and Ronn O. 1981 Pharmacokinetics of metoprolol in patients with hepatic cirrhosis *Clin. Pharmacokinet.* 6 375-88.

Remmel R. P., Copa A. K., Angaran D. M. 1991. The effects of hemodilution, pH and protamine on lidocaine plasma protein binding and red blood-cell uptake in vitro. *Pharm. Res.* 8:127-130.

Roberts M. S. and Rowland M. 1986. A Dispersion Model of Hepatic Elimination: 1. Formulation of the Model and Bolus Considerations *J. Pharmacokin. Biopharm.* 5 227-60.

Roberts M. S. and Rowland M. 1986. Correlation between in-vitro microsomal enzyme activity and whole organ hepatic elimination kinetics: analysis with a dispersion model *J. Pharm. Pharmacol.* 38 177-81.

Smye S. W., Evans C. J., Robinson M. P. and Sleeman B. D. 2007. Modelling the Electrical Properties of Tissue as a Porous Medium *Phys. Med. Biol.* 52 7007–22.

Shibata Y., Takahashi H., Chiba M. and Ishii Y. 2002. Prediction of hepatic clearance and availability by cryopreserved human hepatocytes: an application of serum incubation method *ASPET* 30 892-96.

Swift G., Homeida M., Halliwell M. and Roberts C. J. 1978. Antipyrine disposition and liver size in the elderly *Europ. J. Clin. Pharmacol.* 14 149-52.

Willmann S. and Edginton A. N. 2007. Dynamically simulating the interaction of midazolam and the CYP3A4 inhibitor itraconazole using individual coupled whole-body physiologically-based pharmacokinetic (WB-PBPK) models *Theor. Biol. Med. Model* 4 1-1.

Wing L. M., Miners J. O., Birkett D. J., Foenander T., Lillywhite K. and Wanwimolruk S. 1984. Lidocaine disposition–sex differences and effects of cimetidine *Clin. Pharmacol. Ther.* 35 695-701.

Zhou X., Lu T., Wei Y. and Chen X. 2007. Liver Volume Variation in Patients with Virus-Induced Cirrhosis: Findings on MDCT *Am. J. Roentgenology* 189 153-59.

CHAPTER 3

GENERAL DISCUSSION

3.1 Introduction

A better insight to the body processes and a significant cost reduction in pharmaceutical industries can be facilitated by physiological models that integrate the mechanisms associated with pharmacokinetics (PK) and pharmacodynamics (PD) processes. The hepatic drug elimination process the efficiency of which is described by hepatic clearance s is considered as a major PK process that reduces the plasma drug concentration particularly for lipophilic drugs. Several physiological models including well-stirred (WS), distributed sinusoidal perfusion (DSP), parallel tube (PT), dispersion (DP), interconnected tube (ICT), and tank-in series models have been developed to describe the hepatic elimination process. Simplifications and assumptions made to develop and solve models are the major sources of uncertainties of predictions. To improve the predictability of a mechanistic model for hepatic drug elimination, the mathematical formulation must be consistent with the physiological and physical phenomena taking place in the liver. An ability to make robust predictions of drug elimination by the liver requires a mechanistic model that simulates real physiological events in the liver.

Since the liver tissue is inherently porous and highly perfused, a porous media approach can be a promising approach towards analyzing the hepatic drug elimination process. Thus, local volume averaging (LVA) method was used for developing a governing equation to describe the

drug concentration gradient across the liver and to predict hepatic clearance and bioavailability. The predictability of the mechanistic model was evaluated and then the model was employed to perform sensitivity analyses of the hepatic drug elimination process at different conditions. The objective of this chapter is to integrate findings of this study, to discuss the limitations of the proposed model and to suggest future efforts for improving the model.

3.2 Porous media physiological model

In order to apply LVA method to a porous medium, the LVA validity condition must be evaluated according to the porous medium length scales. The length scales of the liver, Brinkman screening length of hepatocytes (5.7×10^{-7} m) (Smye et al., 2007), sinusoidal diameter (6×10^{-5} m) (Zhou et al., 2007), the linear size of an acinus (6×10^{-4} m) (Smye et al., 2007), and the liver equivalent length (2×10^{-1} m) (Zhou et al., 2007), satisfied the validity condition of Eq. (2.2) (Kaviany, 1995) as $5.7\times10^{-7}<<6\times10^{-5}<6\times10^{-4}<<2\times10^{-1}$ m implying that LVA method was applicable to the liver as a porous medium.

The proposed mechanistic model was able to take into account liver porosity, tortuosity, permeability, unbound drug fraction, hepatic tissue partition coefficient, drug-plasma diffusivity, axial/radial dispersion and nonlinear hepatocellular metabolism parameters for describing the drug concentration gradient across the liver and predicting hepatic clearance and bioavailability. A mesh and time step size sensitivity analyses revealed that 350 nodes at a time step size of 1 s were adequate for sufficiently high accuracy and consistency with a reasonable speed of solution. In order to validate the model, the predicted results were compared to the values of hepatic clearance and bioavailability observed for different drugs with low and high hepatic intrinsic

clearance. As well, the predictability of the proposed model was compared to that of WS, PT and DP models.

3.2.1 Validating the proposed model

The predicted values of hepatic clearance and bioavailability were compared to the observed values reported by Shibata et al. (2002) for naloxone, verapamil, phenacetin, lidocaine, metoprolol, caffeine, timolol and diazepam at the hepatic perfusion rate of 1500 $mlmin^{-1}$ for a 70 kg male subject. A coefficient of determination of 0.91 indicated a very good agreement between predictions and observations of the hepatic clearance; however, the model underestimated the hepatic clearance of timolol and verapamil and overestimated the hepatic clearance of phenacetin. The underestimation of the hepatic clearance of timolol may be associated with the genetic polymorphism of timolol hepatocellular metabolism which can cause significant variability in the population (Volotinen et al., 2007). Since the PK properties used in the simulation were not population based, an inherent uncertainty was induced in the estimations of the hepatic clearance of timolol. The large interindividual differences (more than five fold) in oral area under the curve (AUC) of verapamil (Eichelbaum et al., 1981a; Eichelbaum et al., 1981b; Lin and Lu, 2001) could have a significant contribution to the uncertainty of the estimations of intrinsic clearance of verapamil, which was used for the simulation in this study. Since the hepatic clearance is very sensitive to the variation of intrinsic clearance (Fig. 2.10a), the uncertainty of the intrinsic clearance of verapamil due to the large interindividual variability, can be the potential source of uncertainty in the estimation of hepatic clearance of verapamil.

The proposed model predicted bioavailability well showing a relatively good agreement with observed values with a coefficient of determination of 0.80. Since the bioavailability was calculated based on the hepatic clearance, Eq. (2.19), the uncertainty associated with the estimated hepatic clearance propagated into the predicted bioavailability values. In addition, the

reported values were based on oral bioavailability while the proposed model could estimate only the hepatic bioavailability. Therefore, lacking the information of drug loss in the intestine and portal vein, predicted values of bioavailability inherently had a discrepancy with the observed values of oral bioavailability.

3.2.2 PM model predictability compared to WS, PT and DP models

The proposed PM model indicated smaller mean square prediction error (MSE) for hepatic clearance predictions compared to WS, PT and DP models. The physiologically oversimplified WS model led to significantly larger MSE in hepatic clearance predictions. MSE values of bioavailability predictions were similar for PM, PT and DP models while WS model resulted in larger MSE. All models indicated very close coefficient of determination values for hepatic clearance as well as bioavailability. Also, all coefficient of determination values for the hepatic clearance were larger than those for bioavailability. Since the proposed numerical model takes into account more structural (i.e. porosity, tortousity) and physico-chemical parameters (i.e. tissue partition coefficient) compared to the other models, more errors associated with the parameters were expected to eventually appear in the predictions. However, despite several mechanistic parameters in the model, the proposed model resulted in smaller MSE with similar coefficient of determination for predicted values of hepatic clearance compared to WS, PT and DP models. This analysis suggests a potential improvement in predictability of the hepatic drug elimination if a porous media approach is adopted.

3.3 Simulation and sensitivity analyses

One of the applications of the validated model is to simulate the drug concentration distribution profile across the liver. Also, the proposed model was used for assessing the

sensitivity of the hepatic drug elimination process to drug physico-chemical properties as well as liver physiological parameters and the transport properties.

3.3.1 The effect of axial dispersion on the drug distribution profile

Simulation results indicated that axial dispersion has a significant effect on drug distribution across the liver. Unlike advection and diffusion, axial dispersion causes the drug to be distributed along the liver within seconds. In the absence of dispersion effect, it takes the drug about 20 s to reach the hepatic vein at the liver outlet; however, with an axial dispersion number of 0.17, the drug reaches the hepatic vein within less than 10 s. Axial dispersion causes the drug to experience less residence time which causes an inadequate time for the drug to reach equilibrium with hepatocytes, which, in turn, can reduce the first pass effect within the initial distribution time. For high extraction ratio drugs which are highly extracted as passing through the liver, the delay in plasma-tissue equilibrium caused by the axial dispersion can significantly enhance the bioavailability of the drug. In addition, when only diffusion and advection are the major transport mechanisms of the drug in the liver, the maximum drug concentration gradient across the liver remains high during the distribution time. In contrast, in the presence of dispersion effect the maximum drug concentration gradient is low.

3.3.2 The influence of the liver porosity on the liver drug distribution profile

Simulation results for different levels of the liver porosity revealed that an increase in the liver porosity decreases the plasma drug concentration gradient across the liver and vice versa for decreasing the liver porosity. The simulation indicated that the influence of the porosity on the drug distribution in the liver can be attributed to the variation of sinusoidal blood velocity (pore velocity) with porosity. Lower sinusoidal porosity leads to higher pore velocity enhancing the effect of the advection. Larger advection effect leads to a faster drug movement towards the

hepatic vein such that the residence time is reduced and the drug concentration at any position across the liver increases during the transient distribution time.

3.3.3 The effect of tissue partition coefficient on the liver drug distribution profile

Simulation of drug distribution across the liver at different values of hepatic tissue partition coefficient indicated that larger tissue partition coefficient values lowered the plasma drug concentration for all positions along the liver at all distribution times. It was physiologically consistent with the fact that the drug is partitioned into the liver tissue when the partition coefficient increases. Indeed, larger partition coefficient reduces the plasma drug concentration as more drug is partitioned into hepatocytes. Simulation analysis also revealed that once drug distribution in the liver reached steady state where the plasma concentration did not change with time across the liver, the role of hepatic tissue partition coefficient became insignificant.

3.3.4 The sensitivity of liver drug distribution profile to intrinsic clearance

Simulation of hepatic drug elimination indicated that as the intrinsic clearance increased from very low to low values (from 0.05 to 0.15 $Lmin^{-1}$), the plasma drug concentration gradient along the liver increased dramatically. When the intrinsic clearance was increased further (greater than 0.2 $Lmin^{-1}$), the plasma drug concentration in the second half of the liver approached zero. It implied that the entire drug was eliminated while traveling through the liver if the intrinsic clearance is greater than 0.2 $Lmin^{-1}$. Consequently, unlike the second half of the liver, the first half of the liver was found to be more sensitive to high intrinsic clearance values.

3.3.5 The sensitivity of liver drug distribution profile to unbound fraction

The plasma drug concentration gradient increased with unbound fraction; however, the sensitivity of plasma drug concentration to the unbound fraction was not as significant as that to the intrinsic clearance. The unbound fraction values greater than 0.8 led to significantly low plasma drug concentration at the last 2 cm of the liver.

3.3.6 The sensitivity of hepatic clearance to perfusion rate and intrinsic clearance

The sensitivity analysis of hepatic clearance with respect to the perfusion rate and intrinsic clearance indicated that for low values of the intrinsic clearance (from 0.01 to 0.1 $Lmin^{-1}$ kg^{-1}), hepatic clearance was not sensitive to the perfusion rate but highly sensitive to the intrinsic clearance. As the value of the intrinsic clearance increased, the hepatic clearance was more sensitive to the perfusion rate and less sensitive to the intrinsic clearance. This suggests that at higher values of intrinsic clearance the speed of drug presentation to the hepatocytes that is determined by perfusion rate is the limiting factor for hepatic clearance which is consistent with other model predictions (i.e. WS, DP models).

3.3.7 The sensitivity of bioavailability to perfusion rate and intrinsic clearance

The hepatic bioavailability was found to be very high at low intrinsic clearance for all levels of perfusion rate. As intrinsic clearance increased, bioavailability decreased dramatically such that for intrinsic clearance values greater than 0.2 $Lmin^{-1}kg^{-1}$ bioavailability approached zero implying the entire drug is metabolized by the liver during its first pass across the liver. Although bioavailability was slightly sensitive to the perfusion rate at high intrinsic clearance (less than 0.2 $Lmin^{-1}kg^{-1}$), the influence of intrinsic clearance on bioavailability was predominant over the perfusion rate. The sensitivity analysis results had a very agreement with the predictions from WS, PT and DP models indicating the validity of PM model predictability.

3.3.8 The influence of unbound fraction and intrinsic clearance on bioavailability

For very low unbound fraction (i.e. <0.1) or intrinsic clearance (i.e. <0.1 $Lmin^{-1}kg^{-1}$) bioavailability gradually decreased with unbound fraction or intrinsic clearance. When unbound fraction and intrinsic clearance were very low, an increase in only one caused no substantial drop in bioavailability due to the suppressing effect of the low value of the other variable. However, for higher unbound fraction (i.e. >0.15) and intrinsic clearance (i.e. >0.15 $Lmin^{-1}kg^{-1}$), any

increase in the either unbound fraction or intrinsic clearance induced a significant drop in bioavailability indicating that hepatocellular metabolism was sensitive to the magnitude of unbound fraction and intrinsic clearance. Other models suggest the same results as the simulation results from PM model. Bioavailability approached zero when unbound fraction and intrinsic clearance were greater than 0.5 and 0.2 $Lmin^{-1}kg^{-1}$, respectively.

3.3.9 Simulation of hepatic drug elimination with nonlinear intrinsic clearance

Simulation revealed an exponentially increasing trend of the intrinsic clearance along the liver for all time points during transient drug distribution in the liver. The variation of concentration dependent intrinsic clearance was consistent with the decreasing trend of plasma unbound drug concentration gradient as well as the intrinsic clearance function (Eq. (2.9)). The drug concentration across the liver increased with time causing intrinsic clearance to decrease according to the intrinsic clearance function, Eq. (2.9). As the drug distribution in the liver approached steady state in which the plasma drug concentration remained unchanged with time across the liver, the change in the intrinsic clearance remained insignificant; however, the intrinsic clearance had a nonlinear variation across the liver at all times. In addition, the simulation results indicated that if the affinity term of a drug (i.e. 1'-hydroxymidazolam) is comparable to the lowest drug concentration in the liver (i.e. K_M is equivalent to C_u), the fact of concentration-dependent intrinsic clearance must be taken into account for simulation of hepatic drug elimination.

3.4 General conclusions

The proposed porous media approach was successfully evaluated and applied for modeling of drug elimination by the liver. In addition to mass transport and physico-chemical properties,

some structural properties of the liver including tortuosity and porosity were effectively included in the model. It was demonstrated that the LVA method was valid for modeling the hepatic drug elimination process. Unlike WS, PT, ICT, DP, and tank-in-series models, the proposed PM model demonstrated a successful ability to simulate hepatic drug elimination with concentration-dependent intrinsic clearance. Compared to WS, PT and DP models, the proposed model resulted in lower MSE values associated with the hepatic clearance prediction. It suggested an improvement in model predictability for hepatic clearance. A very good agreement between predicted results from PM model and observations as well as the predictions from WS, PT and DP models indicated that the reliability of the application of a porous media viewpoint to analysis of the hepatic drug elimination process.

Excluding the axial dispersion from a model (i.e. WS and PT) inherently causes uncertainty in model predictions. Porosity also influenced the sinusoidal blood velocity such that an increase in liver porosity caused a reduction in plasma drug concentration across the liver. Although the influence of unbound fraction on the drug concentration gradient is appreciable, the effect of intrinsic clearance was significantly higher than the unbound fraction. The influence of perfusion rate on the hepatic clearance became distinctive at larger values of intrinsic clearance while no limiting effect of the perfusion rate was observed at low intrinsic clearance. Also, sensitivity analysis revealed that the bioavailability was sensitive to the interaction between unbound fraction and intrinsic clearance. In addition, the uncertainty associated with the assumption of a constant intrinsic clearance can be avoided if PM model is employed.

3.5 PM model limitations and future studies

A departure from reported observations may exist if the diffusional mass transfer resistance

across the hepatocellular membrane is higher than convection mass transfer resistance. This situation violates the assumption of a local equilibrium in the differential element resulting in significant error in the predictions. The assumption of local equilibrium represented by the tissue partition coefficient also precludes addition of the role of transporters and their potential contribution as a rate-limiting process in the intrinsic clearance of drugs.

The proposed model can be coupled with an absorption model in order to provide a dynamic simulation of the hepatic elimination process following an oral administration. Furthermore, the model can be coupled with models of major body organs (i.e. kidneys, brain, lungs, gastro intestine, muscles) such that the whole body PK can be explored. Then the whole body PK will be used for a better transition from preclinical studies (animal studies) to clinical studies where the model can be applied for investigating the optimum dose. As well, the model will contribute to better understanding different factors affecting the overall disposition (i.e. rate limiting parameters).

The model's ability to describe the time dependent drug concentration with position across the liver makes the model potentially useful for investigating the effect of a pathological deficiency (i.e. shunting) on the pattern of drug distribution across the liver. Part of the liver tissue can be virtually disabled in the model by defining the starting and ending positions associated with shunting. In this way, the defined location will not contribute the hepatic metabolism of the drug as the blood flow and enzyme activity attributed to the location are set to zero in the model. In addition, the model can potentially accommodate the zonal distribution of Phase I and Phase II enzymes in liver acini if solved two dimensionally. Three zones with appropriate boundary conditions can be defined along *y* direction of the liver geometry while three enzymatic activity characteristics (i.e. intrinsic clearance, affinity term, maximum metabolism rate capacity) are

specified to each zone. Two dimensional solution of the model will take into account the zonal effects on the hepatic dug elimination.

Future refinements of the model will address the incorporation of mass transfer resistance associated with transporters and mass diffusion across the hepatocellular membranes. In addition, intrinsic average properties can be used for developing a set of two coupled governing partial differential equations for hepatocytes and blood flow such that the surface area of sinusoids in acini, mass transfer resistance in space of disse, and the drug concentration gradient across hepatocytes and sinusoids are taken into account.

References:

Eichelbaum M., Dengler H.J., Somogyi A. and Van Unruh G.E. 1981a. Superiority of stable isotope techniques in the assessment of bioavailability of drugs undergoing extensive first-pass elimination:studies of the relative bioavailability of verapamil tablets. *Eur. J. Clin. Pharmacol.* 19:127–131.

Eichelbaum M., Somogyi A., Van Unruh G.E. and Dengler H.J., 1981b. Simultaneous determination of the intravenous and oral pharmacokinetic parameters of D,L-verapamil using isotope-labeling verapamil. *Eur. J. Clin. Pharmacol.* 19:133–137.

Kaviany M. 1995. *Principles of Heat Transfer in Porous Media*, second ed., Springer, New York.

Lin J.H. and Lu Y.H.A. 2001. Interindividual variability in inhibition and induction of cytochrome P450 enzymes. *Annu. Rev. Pharmacol. Toxicol.* 41:535–567.

Smye S.W., C.J. Evans, M.P. Robinson and B.D. Sleeman. 2007. Modelling the Electrical Properties of Tissue as a Porous Medium. *Phys. Med. Biol.* 52: 7007–7022.

Volotinen M., M. Turpeinen, A. Tolonen, J. Uusitalo, J. Mäenpää, O. Pelkonen. 2007. Timolol Metabolism in Human Liver Microsomes Is Mediated Principally by CYP2D6. *Drug Metab. Dispos.* 35: 1135–1141.

Zhou X., T. Lu, Y. Wei and X. Chen. 2007. Liver Volume Variation in Patients with Virus-Induced Cirrhosis: Findings on MDCT. *Am. J. Roentgenol.* 189: 153–159.

APPENDIX:

Discretized equations of the partial differential governing equation (Eq. 2.8)

Node i=1:

As the node 1 is subjected to irregular boundary, the non-uniform grid size based finite difference must be applied to the governing equation. The tailor's series expansion of variable *C* at node *i+1* with a node size of *Δx,* and at node *i-1* with a node size of *Δx/2* are given as:

$$C_{i+1}^{j} = C_i^j + \Delta x \left.\frac{\partial C}{\partial x}\right|_i + \Delta x^2 \frac{1}{2!}\left.\frac{\partial^2 C}{\partial x^2}\right|_i \quad \text{for a node size of } \Delta x$$

$$C_{i-1}^{j} = C_i^j - \frac{\Delta x}{2}\left.\frac{\partial C}{\partial x}\right|_i + \frac{\Delta x^2}{4}\frac{1}{2!}\left.\frac{\partial^2 C}{\partial x^2}\right|_i \quad \text{for a node size of } \frac{\Delta x}{2}$$

Multiplying the first equation by 1/2 and adding the result to the second equation results in:

$$\begin{cases} \frac{1}{2}\left(C_{i+1}^{j} = C_i^j + \Delta x \left.\frac{\partial C}{\partial x}\right|_i + \Delta x^2 \frac{1}{2!}\left.\frac{\partial^2 C}{\partial x^2}\right|_i \right) & \text{for a node size of } \Delta x \\ C_{i-1}^{j} = C_i^j - \frac{\Delta x}{2}\left.\frac{\partial C}{\partial x}\right|_i + \frac{\Delta x^2}{4}\frac{1}{2!}\left.\frac{\partial^2 C}{\partial x^2}\right|_i & \text{for a node size of } \frac{\Delta x}{2} \end{cases}$$

$$\frac{C_{i+1}^{j}}{2} + C_{i-1}^{j} = \frac{C_i^j}{2} + C_i^j + \frac{\Delta x}{2}\left.\frac{\partial C}{\partial x}\right|_i - \frac{\Delta x}{2}\left.\frac{\partial C}{\partial x}\right|_i + \frac{\Delta x^2}{4}\left.\frac{\partial^2 C}{\partial x^2}\right|_i + \frac{\Delta x^2}{8}\left.\frac{\partial^2 C}{\partial x^2}\right|_i$$

Rearranging the result for the second derivative term leads to the approximation of the second derivative of *C* with respect to *x* with non uniform grid sizes of *Δx* and *Δx/2* as:

$$\left.\frac{\partial^2 C}{\partial x^2}\right|_i = \left(\frac{8}{3\Delta x^2}\right)\left(\frac{1}{2}C_{i+1}^{j} - \frac{3}{2}C_i^j + C_{i-1}^{j}\right) = \left(\frac{16}{3\Delta x^2}\right)\left(C_{i+1}^{j} - 3C_i^j + 2C_{i-1}^{j}\right)$$

If the above equation is applied to the diffusion term in Eq. (2.8), and the convection term is discretized using backward finite difference, the discretized form of Eq. (2.8) based on implicit finite difference with non uniform grid size at the boundary will be as:

$$\frac{(1-\varepsilon)K^* + \left(\frac{\varepsilon}{f_{u(B)}}\right)}{\Delta t}\left(C_1^j - C_1^{j-1}\right) = \frac{16\left(\frac{D_{AB}\varepsilon}{\tau}\right)}{3\Delta x^2}\left(C_2^j - 3C_1^j + C_{x=0}^j\right) - \frac{2\overline{u}_B}{f_{u(B)}\Delta x}\left(C_1^j - C_{x=0}^j\right)$$
$$- Cl_{\text{int}} C_i^j$$

Nodes $1 < i \leq N$:

Applying central finite difference to the diffusion term and backward finite difference to the convection term results in the discrete form of Eq. (2.8) for nodes 2 to *N* as:

$$\frac{(1-\varepsilon)K^* + \left(\frac{\varepsilon}{f_{u(B)}}\right)}{\Delta t}\left(C_i^j - C_i^{j-1}\right) = \frac{\left(\frac{D_{\parallel}^d}{f_{u(B)}} + \frac{D_{AB}\varepsilon}{\tau}\right)}{\Delta x^2}\left(C_{i+1}^j - 2C_i^j + C_{i-1}^j\right) - \frac{\overline{u}_B}{f_{u(B)}\Delta x}\left(C_i^j - C_{i-1}^j\right)$$
$$- Cl_{\text{int}} C_i^j$$

Node i=N+1:

Defining a fictitious node of *N+1* at the outlet (the second boundary) and applying no-diffusion mass flux condition, the algebraic finite difference equation at the virtual node of *N+1* will be as:

$$\frac{(1-\varepsilon)K^* + \left(\frac{\varepsilon}{f_{u(B)}}\right)}{\Delta t}\left(C_{N+1}^j - C_{N+1}^{j-1}\right) = \frac{\left(\frac{D_{AB}\varepsilon}{\tau}\right)}{\Delta x^2}\left(2C_N^j - 2C_{N+1}^j\right) - \frac{\overline{u}_B}{f_{u(B)}\Delta x}\left(C_{N+1}^j - C_N^j\right)$$
$$- Cl_{\text{int}} C_{N+1}^j$$

Where:

$$Cl_{\text{int}} = \begin{cases} Cl_{int-invivo} & \text{if } Cl_{\text{int}} \neq f(C) \\ \dfrac{V_{\max}}{K_M + C_i^{j-1}} & \text{if } Cl_{\text{int}} = f(C) \end{cases}$$